Analysis of shape uses local apparent position rather than physical position

J. Edwin Dickinson School of Psychological Science, University of Western Australia, Crawley, Perth, Western Australia, Australia

Ken W. S. Tan School of Psychological Science, University of Western Australia, Crawley, Perth, Western Australia, Australia; Visual Neuroscience Group, School of Psychology, The University of Nottingham, Nottingham, UK

David R. Badcock School of Psychological Science, University of Western Australia, Crawley, Perth, Western Australia, Australia

Objects are often identified by the shapes of their boundaries. Here, by measuring threshold amplitudes for detection of sinusoidal modulation of local position, orientation and centrifugal speed in a closed path of Gabor patches, we show that the positions of such boundaries are misperceived to accommodate local illusions of orientation context and motion induced positional bias. These two types of illusion are shown to occur independently, but the misperception of position is additive. We conclude that, in the analysis of shape, the visual system uses the apparent rather than the veridical boundary conformation.

Introduction

Objects in the visual environment are the targets for our thoughts and actions and are often identified by the shapes of their boundaries (Biederman & Ju, 1988; Kourtzi & Kanwisher, 2000). However, the perceived shape of an object is elastic, being susceptible to the effects of its spatial and temporal context. Some contextual effects, for example those pertaining to size and aspect ratio, appear to act at the level of analysis of the shape of the object (Dickinson, Green, Harkin, Tang, & Badcock, 2019; Dickinson, Morgan, Tang, & Badcock, 2017; Regan & Hamstra, 1992). The perceived shape of an object is, however, also influenced by contextual effects that act more locally. Local effects of orientation context, for example, have been shown to influence perceived shape (Bowden, Dickinson, Green, & Badcock, 2019; Dickinson, Almeida, Bell, & Badcock, 2010; Dickinson & Badcock, 2013; Dickinson, Mighall, Almeida, Bell, & Badcock, 2012). Under certain conditions, local contextual effects can also lead to the misinterpretation of the configuration of a path. The Fraser illusion (Fraser, 1908), for example, illustrates the systematic misperception of the local orientation of a path caused by the finer-scaled structure, or local orientation content, being incongruent with the orientation of the path. The illusion is also known as the twisted cord illusion, with the perceived local orientation of the path displaced toward the orientation defined by the twist in the cord used to depict the path. A particularly impressive manifestation of the twisted cord illusion is known as the Fraser spiral, which describes the condition in which a set of concentric circular paths are perceived as a spiral. A simple illustration of the Fraser spiral is shown in the top left panel of Figure 1. The pattern shown is comprised of concentric circles of Gabor patches, Gaussian windowed sinusoidal gratings, with the patches arranged such that their axes are rotated away from being tangential to the circles on which they are placed. The local systematic misalignment of the patches relative to the circular paths results in the orientation of the paths of patches being drawn toward the orientation of the patches such that the paths are no longer perceived as circular. The visual system incorporates the misperception of the position of the paths by perceptually reinterpreting them as a spiral.

The perception of the spiral form seen in the example of the Frazer spiral in the top left panel of Figure 1 could arise as a consequence of the misperception of locus of the path required by the visual system's need to accommodate the systematic misperception of its local orientation. This places local position and orientation in competition and raises the question of how local position and orientation cues contribute to

Citation: Dickinson, J. E., Tan, K. W. S., & Badcock, D. R. (2021). Analysis of shape uses local apparent position rather than physical position. *Journal of Vision*, *21*(10):5, 1–26, https://doi.org/10.1167/jov.21.10.5.

https://doi.org/10.1167/jov.21.10.5 Received April 7, 2020; published September 2, 2021 ISSN 1534-7362 Copyright 2021 The Authors

This work is licensed under a Creative Commons Attribution-NonCommercial-NoDerivatives 4.0 International License.

Downloaded from hwmaint.iovs.org on 04/25/2024

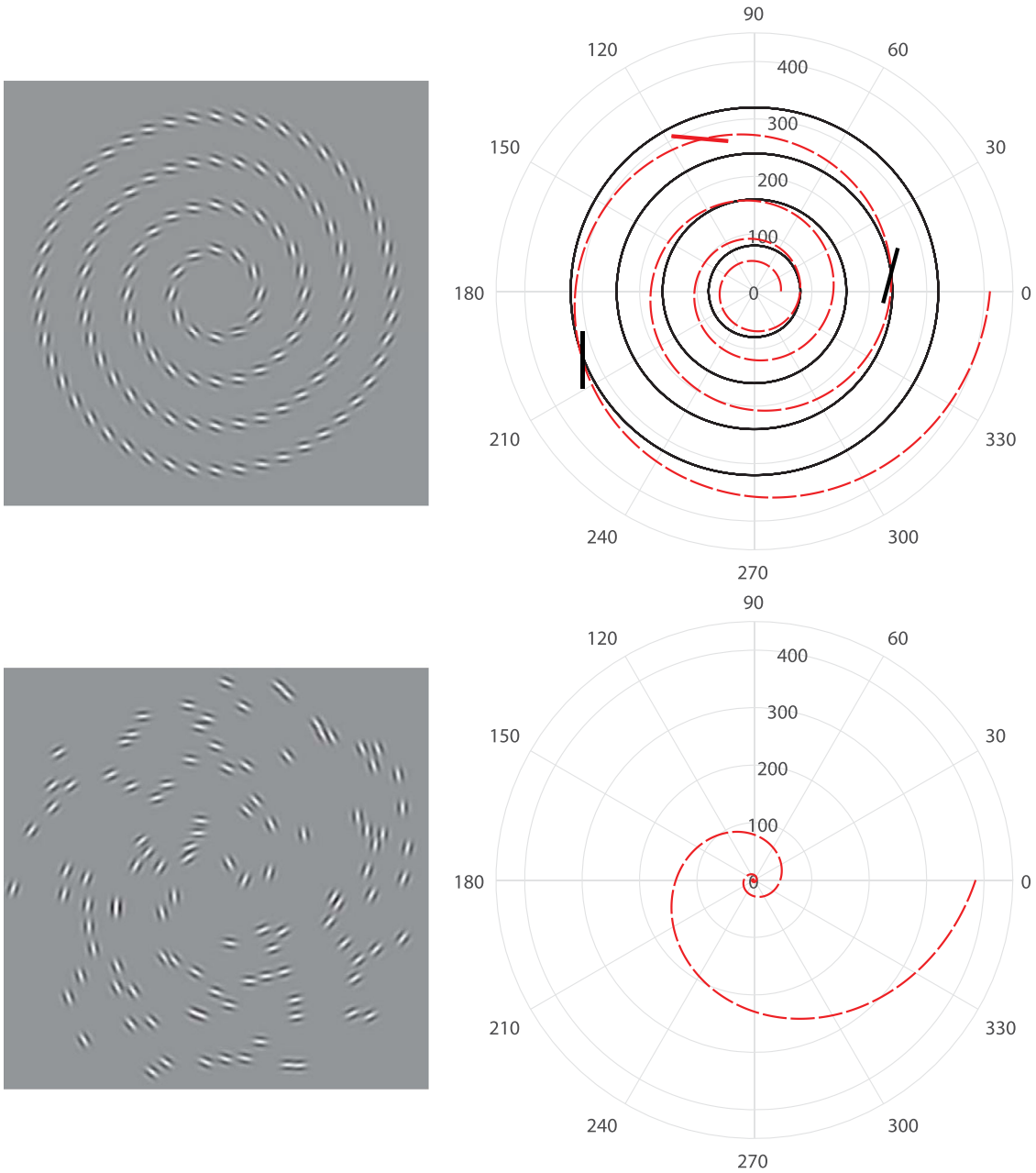

Figure 1. A demonstration of the Fraser spiral (top left) with a conceptualization of the illusion (top right), and an example of a spiral texture (bottom left) and a representation of the spiral form perceived within it (bottom right). Top left, Gabor patches are arranged on concentric circular paths. The circular paths are misperceived as a spiral pattern. Top right, the concentric circles are illustrated as solid black circles, and a logarithmic spiral, illustrating the percept of the spiral form, is superimposed as a dashed red line. Bold, black straight lines intersect the largest and second largest circles at an angle of −20 degrees to the local tangents to the circles. These lines represent the orientations of the Gabor patches relative to the circular paths on which their centers are positioned. Locally, the twisted cord illusion causes the perceived orientation of the path of Gabor patches to be drawn toward that of the axes of the Gabor patches. The magnitude of this effect is a function of the orientation difference between the circular path and the Gabor patches. The angle by which the perceived orientation of a short path of Gabor patches differs from its true orientation peaks at an orientation difference, between the path and the axes of the Gabor patches, of around 20 degrees (Dickinson, Harman, Tan, Almeida, & Badcock, 2012), the difference in orientation used in the demonstration. The dashed red spiral path has an angle of −5 degrees relative to a tangent to a circle along the same radius. The angle of −5 degrees is chosen to illustrate the attraction of the path of Gabor patches towards the angle, of −20 degrees, that the axes of the Gabor patches make with the concentric circular paths of patches. Illusions of this magnitude have been demonstrated in short paths of Gabor patches (Dickinson, Harman, et al., 2012). Bottom left, the Gabor patches have been randomized in radial position to create a texture that is perceived to have a spiral form. A logarithmic spiral that makes an angle of −20 degrees with the perpendicular to the local radius is shown bottom right. The spiral texture, on inspection, appears to have the same pitch as the illustrated logarithmic spiral.

Downloaded from hwmaint.iovs.org on 04/25/2024

shape perception. This is the question we address in the current study. The conclusion of an earlier study which placed sinusoidal modulation of position and orientation into competition around a closed path was that the position and orientation structure was analyzed independently and globally around the path, with the most reliable cue preferred in the analysis of shape (Day & Loffler, 2009). Day and Loffler used a path of Gabor patches, allowing orientation and position of the patches to be varied independently, and comprehensively measured the effects of sampling of the path, where the local Gabor patches represent the samples. Variation of parameters such as the sampling frequency along the path, Gabor carrier frequency, and Gabor envelope size resulted in changes in the relative weighting of the orientation and position information. A global explanation of the effects of orientation modulation within the Gabor patches was adopted in preference to a local solution, in part because the orientation-induced shape was preserved when Gabor scale (size and frequency) and phase were randomized around the path, the argument being that this implied that the shape analysis was performed subsequent to the early analysis of local orientation. Day and Loffler (2009) also argued that the envelopes of the Gabor patches are circular and are, therefore, individually not susceptible to illusions of orientation. These arguments, however, do not include the possibility that the path of patches is perceived as a shape. The fact that the Fraser illusion is known synonymously as the twisted cord illusion illustrates that the path of the cord and its internal orientation structure are both perceived. The orientation of the twist in the cord is defined by the luminance properties of the Gabor patches, whereas the orientation of the cord is defined by the second order envelope (Dakin, Williams, & Hess, 1999). The internal orientation influences the perceived orientation of the cord, rotating the perceived orientation of the envelope of the cord toward that of the twists of the cord. A circular path of Gabor patches with a sinusoidal modulation of orientation from tangential to that path can be considered analogous to the Fraser spiral but with the twist of the cord reversing periodically. The path is then perceived as though it is modulated in radius (Fraser, 1908 contains an illustration of this condition). The example of a spiral texture shown in the panel bottom left shows that a spiral form can be discerned in a pattern comprised of randomly placed but coherently oriented Gabor patches (see Webb, Roach, & Peirce, 2008). The pitch of the spiral in this pattern, however, approximates the angle that the patches make with the perpendicular to the local radius, as demonstrated in the illustration bottom right. There is no continuous path of patches in the example and so the form must be due to a mechanism for processing of texture rather than the shape of a boundary. Sensitivity to spiral textures has also previously been demonstrated in Glass patterns, patterns defined by coherence in polar orientation of pairs of dots (Dickinson & Badcock, 2007; Seu & Ferrera, 2001).

In order to determine if the shape seen in circular paths of Gabor patches modulated in orientation is due to the global analysis of orientation or, instead, to a global interpretation of the form of a path that is subject to the effects of illusions of local orientation context, we will, like Day and Loffler, independently manipulate position and orientation modulation within an otherwise circular path of Gabor patches. In contrast, however, we will use a measure of threshold amplitude for detection of modulation as this more readily lends itself to quantitative analysis of the perceived shape.

The visual system is exquisitely sensitive to deformations of a path from a circle (Loffler, Wilson, & Wilkinson, 2003; Regan & Hamstra, 1992; Wilkinson, Wilson, & Habak, 1998), making measurements of deformation from circular a sensitive measure of visual performance. Patterns with a specific form of deformation from circular, a sinusoidal modulation of radius, have previously been used to demonstrate integration of shape information around closed, continuous paths. These spatial radial frequency (RF) patterns have cycles of sinusoidal modulation, of a fixed wavelength, incrementally added to them until the whole path is modulated by an integer number of cycles of modulation. Patterns with a modulation wavelength of 120 degrees are referred to as RF3 patterns as three cycles of modulation complete the pattern. For patterns where a low number of cycles would complete the whole path (low radial frequency patterns), the rate of decrease in threshold with increasing numbers of cycles of modulation has been shown to be greater than that which can be accounted for by probability summation, the increasing probability of detecting a single cycle as the number of cycles present is increased. This integration of shape information implies a global shape analysis for such patterns (Dickinson, McGinty, Webster, & Badcock, 2012; Green, Dickinson, & Badcock, 2017; 2018a; 2018b; 2018c; Loffler et al., 2003). Of course, in a continuous path, modulation of orientation occurs concomitantly with modulation of position. However, integration has also been demonstrated around Gabor sampled spatial RF patterns (Dickinson, Han, Bell, & Badcock, 2010; Tan, Bowden, Dickinson, & Badcock, 2015; Tan, Dickinson, & Badcock, 2013; 2016a), allowing position and orientation modulation to be introduced independently, which makes them ideal for our purpose. Consequently, in this study, we will introduce low radial frequencies of modulation of position and orientation into paths of Gabor patches. Figure 2 illustrates patterns composed of paths of oriented Gabor patches that have positional and/or orientation modulation.

Downloaded from hwmaint.iovs.org on 04/25/2024

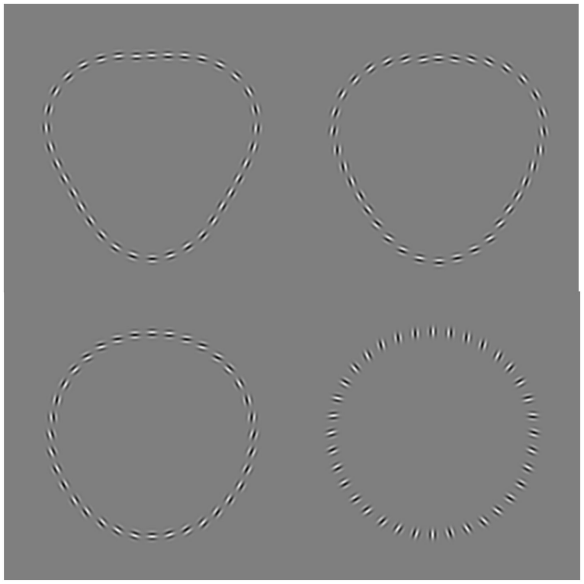

Figure 2. Patterns composed of Gabor patches. The pattern top left comprises Gabor patches distributed around a spatial RF path with the patches aligned tangential to the path. That top right has patches distributed on the same spatial RF path but with the patches aligned perpendicular to the local radius, as would be appropriate for a circle where the patches are aligned with the circle. In the pattern bottom left, the patches are distributed on a circular path, but the patches are aligned as though they were tangent to the spatial RF path. The patches of the pattern bottom right are distributed on a circular path but are modulated in orientation from radial and so the patches are perpendicular to those in the equivalent positions in the pattern to its left.

The effects of the modulation of the positions and orientations of the Gabor patches in a Gabor sampled path are evident in Figure 2. The first three examples are all perceived to have the shape of spatial RF3 patterns, having the appearance of rounded triangles. The triangular shape is most salient in the first pattern (top left) in which the Gabor patches are distributed around a path modulated in position and are arranged tangential to the path such that they are also modulated in orientation. In the second pattern (top right), the patches are distributed on a position modulated path but are arranged perpendicular to the local radius (as would be the case if they were aligned with a circular path). The patches of the third pattern (bottom left) are arranged with their centers on a circle but the patches are oriented as though they were aligned with the position modulated path. In the fourth pattern (bottom right), the patches are perpendicular to those in the pattern to its left, and so the patches can be considered as modulated in orientation from radial. This pattern appears much more circular than the others. Tan et al. (2015) showed that modulation of orientation from radial and concentric in textures composed of Gabor patches was equally salient and so we propose that the shape perceived in the circular path bottom left is due to an illusory distortion to the path due to the twisted cord illusion, which is maximal for a twist in the cord of approximately 20 degrees. The pattern that appears most distorted in Figure 2 is that at the top left, which contains both position and orientation modulation. Dickinson, Harman, Tan, Almeida, and Badcock (2012) have previously shown that that position and orientation modulation both contribute to the perception of shape and that the perceived shape is more salient when the two cues are both present (see Figure 2, top left) than when each is present in isolation (see Figure 2, top right and bottom left). Given that the twisted cord illusion generalizes to a variety of shapes it seems reasonable to propose that the effect is local and acts on perceived orientation of the envelope of the cord.

Dickinson, Harman, et al. (2012) used short lines comprised of three Gabor patches to measure the illusory tilt introduced into a line as a function of the difference in orientation between the Gabor patches and the line they comprise. This allowed the twisted cord illusion to be predicted for any local orientation difference between the Gabor patches and the axis of the line. Thresholds for detection of modulation of orientation around circular paths of Gabor patches were measured and it was shown that, if the illusory misrepresentation of orientation appropriate to the local orientation difference between the patches and the path was applied to the path, and the nominal positions of the patches adjusted to accommodate the apparent local orientations of the path and preserve its continuity, then the amount of illusory positional modulation was sufficient to account for detection of modulation. In Figure 2, the top left pattern is comprised of Gabor patches aligned tangential to the path and so is not subject to the twisted cord illusion. In the pattern in the top right, the illusion acts in opposition to the positional modulation of the path and the path appears less deformed from circular than the pattern to its left. In the pattern bottom left the illusion acts to induce the percept of modulation in a circular path of Gabor patches aligned as though they are tangential to a modulated path (as also shown by Day & Loffler, 2009).

We will adopt the hypothesis that the shape percept is formed through the analysis of the form of the envelope of the perceived path of the Gabor patches, rather than the physical path, and that the form of the path is defined through interpolation of the perceived positions of the patches, which are modified to both accommodate the illusory changes to the local orientation of the envelope of the path and to preserve its continuity. As a test of this hypothesis, we examine how the orientation and position cues integrate locally and also how the combined cues integrate around a path. To this end we measure thresholds for detection of position and orientation modulation in Gabor sampled

Downloaded from hwmaint.iovs.org on 04/25/2024

RF patterns as these patterns have previously been used to demonstrate integration of shape information around a closed path.

In order to demonstrate that our hypothesis generalizes to other local processes that result in local displacement of perceived position, we incorporate modulation of centrifugal motion in the gratings of the Gabor patch stimuli. A stationary Gabor patch which contains a moving grating is perceived as displaced in the direction of motion of its contained grating (De Valois & De Valois, 1991) an effect often termed the De Valois effect or motion position illusion. Dickinson, Han, et al. (2010) showed that, for short durations of presentation, the perceived displacement of a patch varies linearly with the speed of the grating and the duration of its presentation, and so a sinusoidal modulation of centrifugal speed has the potential to result in a sinusoidal modulation of the perceived radius of a circular path of Gabor patches. In the same paper, the threshold amplitude of speed modulation in a circular pattern comprised of Gabor patches with moving carrier gratings was found to decrease with increasing number of cycles of modulation at a rate that was greater than predicted by probability summation. The rate of decrease was consistent with that seen for spatial RF patterns, implying a common process, probably that the perceived modulation was the illusory positional displacement due to the De Valois effect. A comparison of the measured De Valois effect in isolated Gabor patches with thresholds for detection of modulation in spatial RF patterns showed that, if applied around a circular path of Gabor patches, the spatial displacement in the path due to the predicted local De Valois effect could account for the observed sensitivity to speed modulation in, so called, motion RF patterns.

Two other previous studies have used motion RF analogs of spatial RF patterns but drew different conclusions to Dickinson, Han, et al. (2010). Rainville and Wilson used Gabor sampled patterns with the speed of the contained gratings modulated sinusoidally from zero (Rainville & Wilson, 2004; 2005). They reported a decrease in threshold with increasing number of cycles of modulation that was steeper than that which would be predicted for a linear summation of signal across cycles. This would require a mechanism that combined information across cycles in a synergistic manner. Dickinson, Han, et al. (2010), argued that the discrepancies between their results and those obtained by Rainville and Wilson were due to differences in the sectors on the motion RF paths defined to be unmodulated. Dickinson, Han, et al. (2010), used patterns with a baseline centrifugal motion to which a sinusoidal modulation of speed was added, and so the unmodulated parts of the patterns simply had the baseline centrifugal speed. Rainville and Wilson modulated radial speed around a speed of zero and permuted the speeds of the patches in the sectors deemed to be unmodulated. A condition of one experiment of Rainville and Wilson (2005) used stimuli in which the modulated sectors appeared predictably at the top of the patterns. For this particular condition, changing the size of the modulated sector had no effect on detection thresholds (see Figure 3 of Rainville and Wilson (2005)). A possible explanation for this result is that such patterns were discriminated from unmodulated patterns through the identification of a region of the pattern within which the speed changed smoothly and gradually. In unmodulated sectors of the patterns, the speeds are locally incoherent and the coherent, or smoothly varying, speeds of the patches comprising modulated sectors might be expected to be highly salient if the observer knows where to look. If the position of the coherent sector were uncertain, then performance might be expected to degrade rapidly with an increasing proportion of the path containing incoherent speeds, thereby accounting for the particularly steep reduction in threshold with an increasing proportion of modulated path. This interpretation is supported by evidence that the thresholds in the conditions where the position of the modulated sector were known and unknown converged when the whole pattern was modulated. Other than in this case, which is essentially identical across the conditions, thresholds for the condition where the position of the modulated sector was known were lower than those where it was unknown. This suggests that the task is performed locally under all circumstances.

We contend, therefore, that the rapid reduction in threshold with an increasing proportion of modulated path seen by Rainville and Wilson is a consequence of the method used to represent the unmodulated sector, and postulate that the modulation perceived in motion RF patterns is the illusory positional modulation that can be attributed to the De Valois effect. This illusory modulation might be expected to add to a genuine modulation of position and any effects of orientation context and provide a test that our hypothesis generalizes. Under such circumstances, we would expect a rate of reduction in the threshold with increasing numbers of cycles of modulation to be comparable to that observed for conventional spatial RF patterns, and demonstrably steeper than probability summation predictions.

The rate of decrease expected to occur due to probability summation reported by Rainville and Wilson and also by Dickinson, Han, et al. (2010) was predicted using the negative inverse of the slope of the psychometric functions, a high threshold theory (HTT) assumption (Wilson, 1980). This method has been recently challenged (Baldwin, Schmidtmann, Kingdom, & Hess, 2016) and it has been replaced by a method using signal detection theory (SDT) estimates of probability summation. This change has not affected previous conclusions with regard to the

Downloaded from hwmaint.iovs.org on 04/25/2024

existence of global shape processing. Although global processing of conventional spatial RF patterns has been demonstrated using probability summation predictions based on SDT (Green et al., 2017; 2018a; 2018c), thus far it has not for Gabor sampled RF patterns. Spatial integration has, however, been demonstrated in RF patterns that also require integration over time (Green et al., 2018b) using these SDT methods.

To summarize, we will use a sensitive measure of shape, the threshold amplitude of modulation in RF patterns, to examine sensitivity to modulation of position, orientation, and centrifugal speed around these patterns. Our central hypothesis is that modulation of orientation and centrifugal speed introduces illusory modulation of position into the RF patterns. We suggest that the illusory modulation in position experienced when orientation is modulated around the patterns is due to the twisted cord illusion and that the De Valois effect causes an apparent modulation of position when centrifugal speed is modulated. If this is shown to be the case, then it is not necessary to invoke the independent global analyses of the local orientation structure present in the gratings of the Gabor patches, as proposed by Day and Loffler (2009), nor radial speed, as proposed by Rainville and Wilson (2004) and Rainville and Wilson (2005) in the analysis of shape.

The size of the twisted cord illusion in a short, straight path of three Gabor patches has been shown to follow a first derivative of a Gaussian function of the difference in orientation between the axes of the Gabor patches and the orientation of the path (Dickinson, Harman, et al., 2012). Such a function can arise from a bias in the population response of a bank of orientation selective cells sensitive to the path of Gabor patches. This could arise if those cells were subject to excitatory input from orientation selective cells sensitive to the Gabor patches with the same orientation preference (Dickinson, Harman, et al., 2012; Tang, Dickinson, Visser, & Badcock, 2015). Such a mechanism is intrinsically local, although its effect might be extrapolated along a path if path continuity is preserved. Hayes (2000), showed that paths of Gabor patches are assembled on the basis of their apparent rather than physical positions when subject to illusory displacements induced by local motion, the De Valois effect (De Valois & De Valois, 1991). As Hayes notes, the fact that the illusory position shift precedes the binding of the path demonstrates that the illusion is local. Following this, we postulate that the form of the envelope of the sampled RF path, containing patches modulated in orientation from tangential to the path, is subject to a local illusion of orientation that implies a misperception of position when incorporated into an extended path.

Similarly, if the patches contain centrifugal motion that is modulated in speed from a baseline centrifugal speed, then the path will be subject to a local motion induced illusion of position and, assuming a smooth path is to be perceived, those changes in position must also be reconciled in the envelope of a continuous path of Gabor patches through a misperception of the form of the path. If these misperceptions of position are induced systematically into a shape, then we might expect perception of the shape to be influenced in a predictable manner. Indeed, it is easy to misinterpret the effects of systematic local differences between stimuli as being due to the effects of a mechanism underlying the global analysis of such stimuli. Dickinson, Almeida, et al. (2010) argued that the distortions seen in circles and Cartesian grids after adaptation to RF patterns and RF distorted grids were consistent with the application of local tilt aftereffects, rather than a global RF distortion of the mapping of the spatial representation of the cortex onto the visual field. The same argument was extrapolated to adaptation to faces (Dickinson & Badcock, 2013; Dickinson, Harman, et al., 2012; Dickinson, Mighall, et al., 2012).

We anticipate that the processing of shape will be shown to use the envelope containing the illusory local positions of the Gabor components of the stimuli thereby demonstrating that the substrate of visual perception at the earliest cortical levels resembles an elastic sheet preserving spatial order (retinotopy) but allowing for some flexibility in perceived distances between points in the visual field. Local misperception of position due to spatial and temporal context have been previously reported (Badcock & Westheimer, 1985a; 1985b; Edwards & Badcock, 2003). If the illusory positional shift precedes the binding of the path and the binding of the path precedes the shape analysis then the shape analysis must use the illusory form of the path. Using RF patterns will allow us to determine whether the illusory positional displacements are incorporated into global shape processing. Moreover, because the twisted cord illusion and the De Valois effect are derived from discrete mechanisms, we expect the orientation and motion induced illusory positional displacements to be additive. Demonstration that this is true would provide strong evidence that apparent local positions, subject to local illusions incorporating displacement of perceived position, are used in the analysis of shape, as they are in the binding of discrete elements into paths.

Methods

Observers

Five psychophysical observers were recruited from the Human Vision Laboratory of The University of Western Australia. Two of the observers are authors J. Edwin Dickinson and Ken W. S. Tan. The remaining

Downloaded from hwmaint.iovs.org on 04/25/2024

three were naïve to the purposes of the study. The observers provided their informed consent prior to their participation. The study was approved by The University of Western Australia's Research Ethics Committee and was conducted according to the tenets of the Declaration of Helsinki.

Apparatus

Custom stimuli were generated using Matlab version 7.2 on a Pentium 4 computer and presented from the frame buffer of a Cambridge Research Systems (CRS Ltd., Rochester, UK) 2/5 visual stimulus generator to a Sony Trinitron CPD-G420 monitor. The active screen area had the linear dimensions 35.75 × 26.80 cm and was populated by 1024 × 768 pixels. At the viewing distance of 120 cm pixels at the center of the screen subtended 1 minute of visual angle. The screen luminance was linearized over an 8-bit range using an Optical OP 200-E photometer (head model number 265) and the CRS Desktop software (CRS Ltd., Rochester, UK). The background luminance of the screen was set to 45 cd/m^2 and the maximum luminance of the stimuli set to 90 cd/m^2. The screen was refreshed at 100 Hz. Testing was completed in a darkened room (background luminance <1 cd/m^2) with the viewing distance maintained by a chinrest. Participants responded using two buttons on a standard computer mouse.

Stimuli

The stimuli were based on RF3 patterns, which are patterns deformed from circular by a sinusoidal modulation of radius with a frequency of three cycles of modulation in 360 degrees. The RF patterns were composed of a path of 36 Gabor patches which were each assigned a position and orientation. For an RF pattern in which the position and orientation are appropriate to describe a continuous path (with no twist in the "cord" implied by the orientation of the patches), the radius at which the patches were presented and their orientations are given by the following two equations:

$$R(\theta) = R_0 (1 + A \sin(3\theta + \varphi)) \quad (1)$$

$$\alpha(\theta) = \theta + \frac{\pi}{2} - \tan^{-1}\left(\frac{3A\cos(3\theta + \varphi)}{R(\theta)/R_0}\right) \quad (2)$$

R_o is the base radius of the distorted circle which in all cases was 135 arc minutes (2.25 degrees) of visual angle. A is the amplitude of modulation of the circle, expressed as a ratio of the amplitude to the base radius. The angle θ is the conventional polar angle (increasing anticlockwise from the x axis) and the angle φ is used to vary the phase of modulation of the pattern on a trial-by-trial basis. For some conditions, the gratings of the Gabor patches were static. In other conditions, the gratings of the patches drifted centrifugally with a speed which is defined by the following equation:

$$S(\theta) = S_0 (1 + A \sin(3\theta + \varphi)) \quad (3)$$

S_0 is a background centrifugal speed of 0.5 degrees of spatial angle per second. The parameter A here is the amplitude of the modulation of speed expressed as a proportion of S_0.

The gratings of the Gabor patches had a spatial frequency of 8 cycles per degree of spatial angle (c/°) and the full width at half height of the Gaussian envelope of the patches was 9.42 minutes of visual angle ($\sigma = 4$ minutes). The patches had a maximum Weber contrast of 1. A motion sequence comprised 12 frames, each persisting for four refreshes of the screen (40 ms). The total duration of the motion and static stimuli was 480 ms. Figure 3 illustrates the construction of the stimuli.

There were, therefore, three different ways in which we could modulate the local properties of the patches that resulted in the percept of an RF pattern.

- Modulation of position (see Equation 1)
- Modulation of orientation (see Equation 2)
- Modulation of speed (see Equation 3)

The amplitude of modulation applied was specified by the value of A in the three equations.

Experimental procedure

Sensitivity to the perceived deformation of the test path from circular was measured using a two-interval forced choice (2IFC) task. Modulated test patterns and circular reference patterns were displayed sequentially in randomized order and the observer was required to indicate which interval contained the test pattern. The method of constant stimuli (MOCS) was used with test patterns of nine amplitudes of modulation used to sample the psychometric function. The amplitudes were chosen to map the full psychometric function plotting proportion of correct identification of the test pattern against modulation amplitude. For every condition, each of the amplitudes of modulation was displayed 60 times across three blocks of trials. The probability of correct response was calculated for each amplitude of modulation and a Quick function fitted (see Equation 4).

$$p(A) = 1 - 2^{-\left(1+\left(\frac{A}{\Delta}\right)^{Q}\right)} \quad (4)$$

Downloaded from hwmaint.iovs.org on 04/25/2024

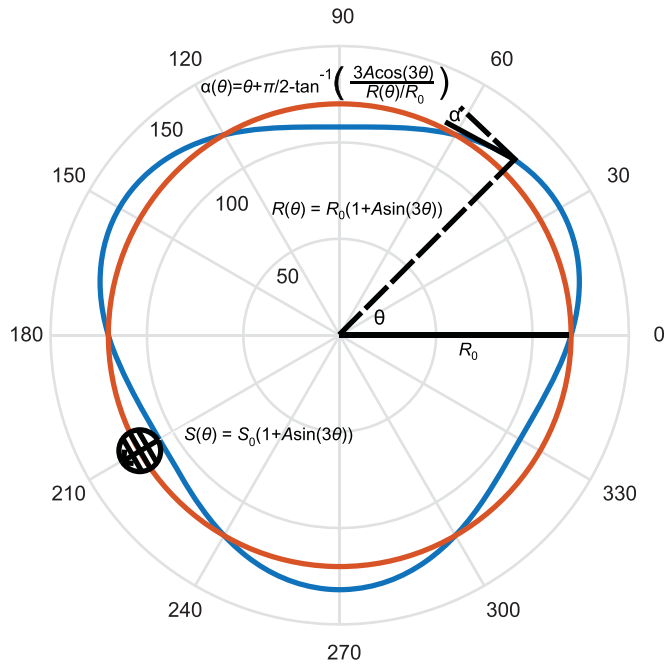

Figure 3. A schematic diagram of the stimulus construction. The red path is circular and the blue path is an RF3 pattern with an amplitude of modulation of radius of 0.1. Stimuli incorporating modulation of position with this amplitude would be comprised of Gabor patches situated on the blue path at a radius $R(\theta)$. If they were also modulated in orientation the axes of the patches would be tangential to this path, at the angle $\alpha(\theta)$ relative to the perpendicular to the local radius. Stimuli with orientation modulation but no modulation of radius would be comprised of patches situated on the red path but with axes at the angle $\alpha(\theta)$ to the path. Stimuli with centrifugal speed modulation would have patches situated on the red path incorporating a grating speed of $S(\theta)$. Stimuli incorporating modulation of position and centrifugal speed modulation would be comprised of patches situated on the blue path and if they also contained orientation modulation the axes of the patches would be aligned tangential to this path, otherwise they would be tangential to a circle. The value of the parameter φ, which defines the orientation of the whole RF pattern, is zero in the example shown above and so, for simplicity, it has been omitted from the equations shown on the diagram.

The nonlinear regression fitting procedure (fitted using Prism) yielded values for the parameter Δ, the threshold for discrimination of the test pattern from the reference circle at a level of 75% correct response, and Q a measure of the slope of the psychometric function. Thresholds for detection of modulation were measured for patterns containing one, two, and three cycles of modulation of each of the position, orientation and motion cues to deformation to determine if integration of these cues could be demonstrated around the patterns. If the illusory positional displacements of the Gabor patches in patterns modulated in orientation and centrifugal speed are treated by the visual system as positional modulation, then their thresholds for detection of modulation can be expected to decrease as cycles of modulation are added at the same rate as for genuine modulation of position. That is, we would expect thresholds to conform to power functions of the number of cycles of modulation present. Moreover, we would expect the indices of the power functions to indicate a rate of decrease in threshold steeper than that predicted by probability summation (Loffler et al., 2003). Further, the thresholds for detection of position, orientation, and speed modulation also allow us to normalize for the relative strength of each cue. The premise for normalization of the amplitudes of modulation is that, if we accept that the modulation of orientation and speed results in local positional modulation, then there exist particular amplitudes of modulation of orientation and centrifugal speed that will induce equal amounts of illusory positional displacement. We chose to express thresholds as the equivalent amount of orientation modulation. Ratios were, therefore, determined to equate threshold amplitudes for single cycles of modulation of position and speed to the threshold for a single cycle of orientation modulation. If these ratios are applied to the amplitudes of modulation of position and speed as normalization constants, then we can apply modulation of orientation, speed, and position in equal effective proportions to a single cycle of modulation and then all three cues to a second and third cycle. Incrementally adding orientation, position and centrifugal speed modulation to a single cycle should have the same effect on threshold as adding positional modulation across three cycles of modulation. Moreover, that effective positional modulation could be divided equally across orientation, position, and centrifugal speed modulation. Thus, if we treat each normalized modulation across a single cycle as a unit cue and incrementally add the cues within and then across cycles of modulation, then the threshold for detection of modulation should decrease according to a power function of the number of cues added. If the cues are integrated equally, then the power function should have an index that exceeds in magnitude that which is predicted by probability summation. Equation 5 specifies a power function.

$$\Delta(n) = Cn^{\gamma} \quad (5)$$

Δ, the threshold, decreases as n increases if the index, γ, of the power function is negative. This is to be expected due to probability summation, the increasing probability of detecting a single cue as the number of independent cues increases. Integration of the signal is demonstrated if the magnitude of γ is greater than that predicted by probability summation. The quantity n, the independent variable in the study, can refer to the number of cycles of modulation

Downloaded from hwmaint.iovs.org on 04/25/2024

or the number of cues. For example, a pattern with orientation and centrifugal speed modulation on a single cycle might be considered to have two cues.

Experiment 1: Uniform centrifugal motion does not mask shape

Integration of shape information has been shown to occur around spatial RF patterns described by continuous, luminance contrast defined paths (Dickinson, McGinty, et al., 2012; Green, et al., 2017; 2018a; Green, Dickinson, & Badcock, 2018b; Green, et al., 2018c; Loffler, et al., 2003). It has also been demonstrated around Gabor sampled paths (Dickinson, Han, et al., 2010; Tan et al., 2015; 2013; Tan, Dickinson, & Badcock, 2016b; Tan, Scholes, Roach, Haris, & McGraw, 2021) although this will be the first study to apply SDT derived estimates of probability summation to such patterns. Integration of speed modulation has also been demonstrated around circular paths (Dickinson, Han, et al., 2010) but again using HTT predictions for probability summation. The effect of a constant centrifugal speed on integration of paths modulated in position and orientation has not been examined. The constant centrifugal motion was introduced to the stimuli so that the test and reference stimulus in the 2IFC task only differed in the degree of modulation introduced to the test stimulus. If there were no constant centrifugal speed, then the reference pattern would be comprised completely of Gabor patches with static gratings. Experiment 1 was conducted to ensure that adding a constant speed to the elements does not substantially alter the ability to detect RF modulation carried by position and orientation cues as in the conventional RF patterns. Movie S1 illustrates the stimulus type used in this comparison between sensitivity to static RF patterns and RF patterns with a constant speed of motion applied to the gratings of the Gabor patches.

Figure 4 shows thresholds for detection of modulation for static patterns and patterns with a constant centrifugal speed for one, two, and three cycles of position and orientation modulation.

Figure 4 shows that adding a constant centrifugal speed to the gratings of the Gabor patches has no effect on the thresholds for detection of position and orientation modulation in Gabor sampled spatial RF patterns. Two-tailed, paired-samples *t*-tests across the indices of the power functions and the logarithms of the multipliers (C) of the fitted power functions showed that they did not differ significantly in either fitted parameter ($t(4) = 0.9179$, $p = 0.3861$ and $t(4) = 1.344$, $p = 0.2501$, respectively). A Bayesian reanalysis (Ly, Raj, Etz, Marsman, Gronau, & Wagenmakers, 2018) assuming a Cauchy prior of 0.707 returns $BF_{10} = 0.547$ and $BF_{10} = 0.736$, respectively, providing support for the hypotheses that the multipliers and indices of the fitted power functions are more likely to be the same across the two stimulus types than different.

The magnitudes of the indices of the power functions were large, indicating a rapid decrease in thresholds for detection of modulation as cycles of modulation were incrementally added. The mean, with 95% confidence intervals, of the indices for the static patterns was -0.76 ± 0.23. For the patterns in motion, it was -0.86 ± 0.22. These results are suggestive of integration of shape information across the cycles of modulation. In order to confirm integration, the indices of the power functions were compared with estimates of probability summation, the increasing probability of detecting a single cycle of modulation as cycles of modulation are incrementally added. Probability summation predictions were calculated according to the principles of SDT using the Palamedes toolbox for Matlab (http://www.palamedestoolbox.org/). The Palamedes routine PAL_SDT_PFML_Fit was used to derive the parameters g and p in the function $d' = gA^p$, describing the discriminability of the stimulus versus stimulus intensity from the single cycle data of each observer using the probabilities of correct identification of the modulated pattern in the 2IFC task. These parameters were then used in the routine PAL_SDT_PS_PCtoSL to predict relative signal levels for one, two, and three cycles of modulation. The use of these functions is described in http://www.palamedestoolbox.org/overview.html and in Prins and Kingdom (2018). Number of cycles of modulation was passed to the routine along with parameters describing the number of choices available to the observer (2 for the 2IFC task), the proportion correct at threshold (0.75) and the number of channels monitored during the task. The number of channels monitored is obviously unknown if the mechanisms by which the local comparisons might be made are unknown, but for the sampled stimuli used in this study it is reasonable to assume that all 36 Gabor patches must be monitored by the observer because the patterns are presented in random phase. It might be argued that for each Gabor patch, multiple orientation and speed channels might provide information independently thereby increasing the number of contributing channels, but increasing the number of channels considered would only make the probability summation predictions less stringent constraints on claims of integration of information around the patterns, so we have used the most conservative test for integration.

A power function was fitted to the probability summation predictions for the signal levels at one, two, and three cycles of modulation. Two-tailed, paired-samples *t*-tests comparing the indices of the power functions fitted to the psychometric data with the indices of the power functions fitted to the probability summation predictions showed that the rate of decrease of the thresholds with increasing numbers of cycles

Downloaded from hwmaint.iovs.org on 04/25/2024

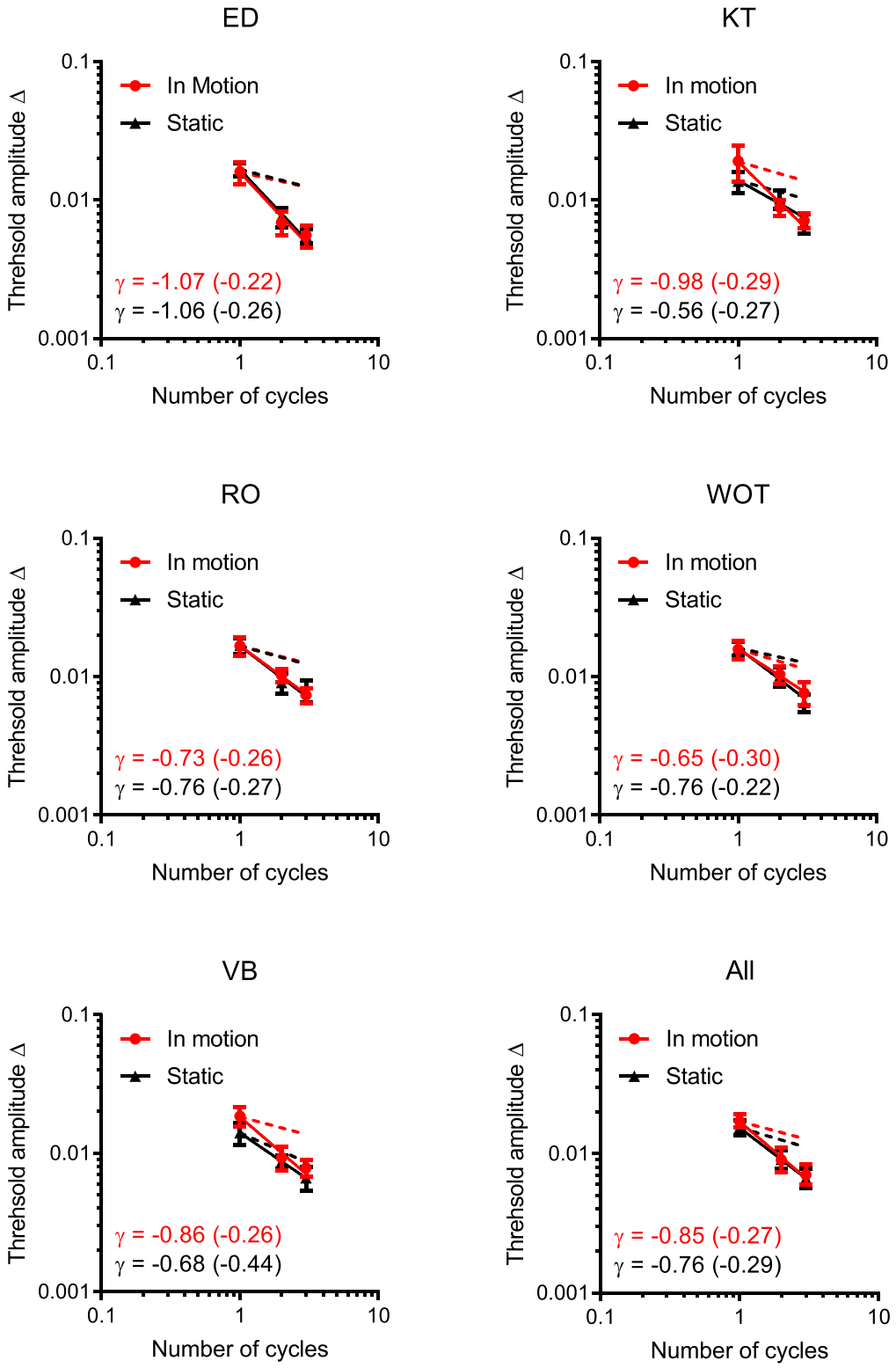

Figure 4. A comparison of modulation detection thresholds across static spatial RF patterns and spatial RF patterns with a constant centrifugal speed around the pattern (no modulation of centrifugal speed). Solid black lines represent power functions fitted to the static pattern thresholds for one, two, and three cycles of modulation of position and orientation. Solid red lines represent power functions fitted to the comparable data for patterns with an added constant centrifugal speed. The graph denoted by *All* plots the geometric means of the thresholds of the individual observers. Error bars indicate the 95% confidence intervals. Dashed black and red lines represent probability summation predictions for static patterns and patterns incorporating centrifugal motion respectively. The indices of the fitted power functions are stated in each of the panels along with, in brackets, the indices of the power functions representing the probability summation predictions as a function of number of cycles of modulation.

Downloaded from hwmaint.iovs.org on 04/25/2024

of modulation exceeded that predicted by probability summation for the static patterns ($t(4) = 4.683$, $p = 0.0094$, $BF_{10} = 7.356$) and for those with a constant centrifugal speed ($t(4) = 6.812$, $p = 0.0024$, $BF_{10} = 19.69$). Figure 4 is annotated with the indices of the power functions fitted to the data of the individual observers. Corresponding indices of power functions fitted to predictions for thresholds conforming to probability summation are shown in brackets.

As the two stimulus types result in the same relationship between thresholds and numbers of cycles of modulation, it was assumed that the RF pattern with constant centrifugal speed could be considered as suitable for measuring sensitivity to modulation of position and orientation independently. These conditions are addressed next.

Experiment 2: Thresholds for position and orientation modulation in RF patterns are consistent with sensitivity to positional modulation incorporating the effects of a local twisted cord illusion

Experiment 2 measured the thresholds for detection of position and orientation modulation when presented individually. Movies S2 and S3 illustrate the stimulus types used. Both stimulus types have a constant centrifugal motion applied to the gratings of the Gabor patches.

Figure 5 plots thresholds for the detection of position modulation and orientation modulation, when presented individually, against the number of cycles of modulation. For comparison, the thresholds for detection of position and orientation when present simultaneously, shown in Figure 4, are reproduced. A comparison between these thresholds and half the value of the geometric mean of the thresholds for detection of position and orientation modulation in isolation is also made.

Figure 5 shows that, at detection threshold, the amplitude of modulation of position and orientation is equal. Two-tailed, paired-samples *t*-tests across the indices (γ) of the power functions and the logarithms of the multipliers (C) of the fitted power functions showed that they did not differ significantly in either fitted parameter ($t(4) = 0.5641$, $p = 0.6028$ and $t(4) = 0.3116$, $p = 0.7709$, respectively). A Bayesian re-analysis of the *t*-tests, assuming a Cauchy prior of 0.707, returned $BF_{10} = 0.452$ and $BF_{10} = 0.414$, respectively, suggesting that the multipliers and indices of the fitted power functions are consistent with being equal across the two stimulus types.

Two-tailed, paired-samples *t*-tests comparing the indices of the power functions fitted to the psychometric data with the indices of the power functions fitted to the probability summation predictions (produced in the same manner as for the previous experiment) showed that the rate of decrease of the thresholds with increasing numbers of cycles of modulation exceeded that predicted by probability summation for the patterns with shape defined by orientation ($t(4) = 6.255$, $p = 0.0033$, $BF_{10} = 15.64$) and for those with shape defined by position ($t(4) = 5.365$, $p = 0.0058$, $BF_{10} = 10.42$).

The patterns modulated in position only have their Gabor patches displaced along an imaginary radial line from the center of the pattern to a point they would occupy if on a spatial RF pattern but are aligned perpendicular to that line (as would be appropriate for a circle). The patterns that are modulated in orientation only have their Gabor patches positioned on a circle but are oriented as though they were on a spatial RF pattern. At any particular amplitude of modulation, the orientation differences between the Gabor patches and the path have the same magnitude across the two pattern types but opposite sign. These differences operate to induce the twisted cord illusion. Locally, the effect of the modulation of this orientation difference around the path due to the twisted cord illusion might then be expected to have the same magnitude but opposite sign. Under such assumptions, the threshold for detection of orientation modulation is the threshold for detection of the twisted cord illusion, with the illusion resulting in a perceived modulation of the path of Gabor patches. The threshold for detection of a position modulated path would be the amplitude of modulation that can be perceived in the presence of the twisted cord illusion acting in the opposite sense. Thresholds for orientation and position modulation might, therefore, be expected to be approximately equal, as we found. A stimulus with position and orientation modulation simultaneously present would not be subject to the twisted cord illusion because the Gabor patches would be aligned tangential to the path. The threshold might then be expected to be half of the threshold for position or amplitude modulation in isolation. The data previously presented in Figure 4 pertaining to position and orientation modulation presented simultaneously is reproduced in Figure 5 in blue. The data presented in green are half the geometric mean of the thresholds for the position and orientation modulation presented in isolation (the data presented in black and red, respectively). Two-tailed, paired-samples *t*-tests across the indices (γ) and the logarithms of the multipliers (C) of the power functions fitted to these data (green and blue lines) showed that they did not differ significantly in either fitted parameter ($t(4) = 0.6106$, $p = 0.5744$, $BF_{10} = 0.461$ and $t(4) = 1.962$, $p = 0.1212$, $BF_{10} = 1.191$, respectively).

Dickinson, Harman, et al. (2012) showed that, at an eccentricity of 2 degrees of visual angle and for small angles of twist in the cord, the twisted cord illusion in a short path of Gabor patches was approximately half of the angle of the twist in the cord (Figure 8 of that paper by Dickinson, Harman, et al. 2012).

Downloaded from hwmaint.iovs.org on 04/25/2024

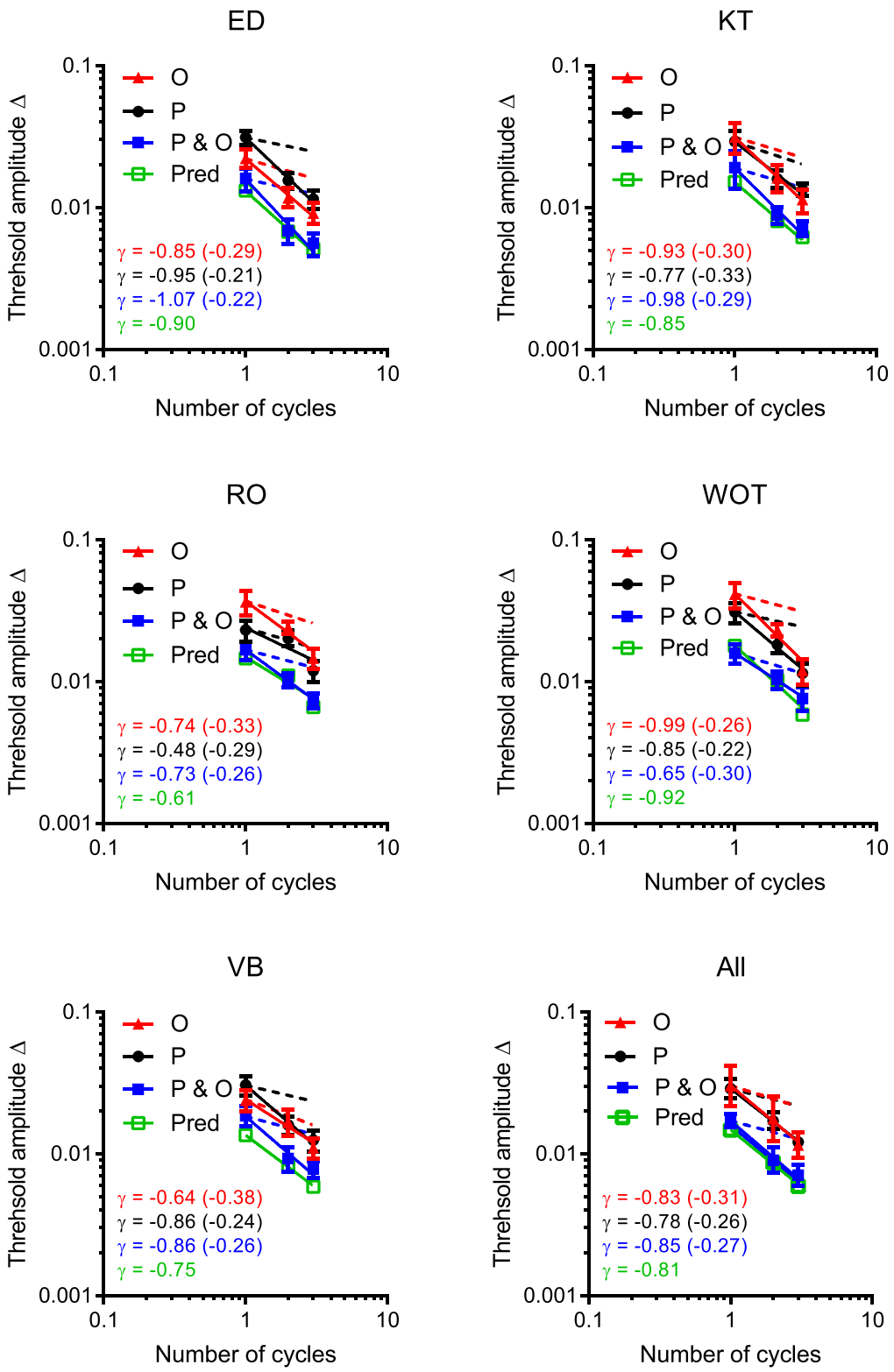

Figure 5. Thresholds for the detection of position modulation and orientation modulation when applied independently and when present simultaneously. Thresholds for the detection of position modulation are plotted for one, two, and three cycles of modulation in black and for orientation modulation in red. Error bars indicate 95% confidence intervals. The data corresponding to stimuli which have both position and orientation modulation (and a constant centrifugal motion) are reproduced from Figure 4 and are plotted in blue. The points rendered in green are values representing half of the geometric means of the data points for position and orientation modulation when presented independently (the data in black and red, respectively). Probability summation predictions are shown as dashed lines and values for the indices of power functions fitted to probability summation predictions are shown in brackets.

Downloaded from hwmaint.iovs.org on 04/25/2024

The single cycle threshold for detection of orientation modulation found here was 0.03, which implies a maximum amplitude of modulation of orientation of 5 degrees. The maximum twisted cord illusion might, therefore, be expected to be 2.5 degrees, which implies a threshold amplitude of modulation for a pattern with positional and orientation modulation (hence no twisted cord illusion) of 0.015. Which is approximately what is found.

We can say, therefore, that the threshold for detection of modulation in RF patterns with both position and orientation modulation is genuinely the amplitude for detection of a modulated path. The threshold for detection of orientation modulation is the threshold for detection of illusory modulation due to the twisted cord illusion, and the threshold for modulation of position is the threshold for detection of perceived modulation in a pattern subject to a competing twisted cord illusion. This supports the hypothesis that it is the perceived local position of a path that is processed in the analysis of shape rather than the actual position or, indeed, independent global analyses of shape through differing local properties, such as position or orientation.

Experiment 3: Thresholds for modulation of centrifugal speed in RF patterns are consistent with sensitivity to positional modulation incorporating the De Valois effect

Extrapolating the hypothesis that local perceived positions are processed in a global analysis of shape, we then investigated the effects of local motion in the De Valois effect on the visual analysis of shape. It has previously been shown that if a path of counter-phasing Gabor patches has the positions of its patches displaced relative to the axis of the path, then the path becomes less salient in noise (Hayes, 2000). The same study showed that if, instead of their envelope being physically displaced, the Gabor patches had a drifting carrier grating that would be expected to displace the perceived positions of the patches such that they became more aligned, then the path became more salient. The conclusion of the study was that the visual system used the perceived local positions in the binding of the path rather than their veridical positions. It is logical, therefore, to assume that it would be the local perceived positions that flowed through to the mechanisms responsible for the analysis of the shape of a path. Of course, not all paths are analyzed globally. Green et al. (2017) demonstrated a global analysis of conventional spatial RF paths, patterns deformed from circular by a sinusoidal modulation of radius, but not lines deformed from straight by a perpendicular sinusoidal modulation of local position. Experiment 3 tests the hypothesis that the perceived positions of Gabor patches that are subject to the De Valois effect are used in the global analysis of shape, rather their physical positions.

In Movies S1, S2, and S3, we can see that the local centrifugal motion of the gratings within the Gabor patches results in an RF pattern appearing to increase in size. If speed is modulated around the pattern, then the pattern can appear to change shape. Dickinson, Han, et al. (2010) showed, for short durations of presentation, that the magnitude of illusory displacement of a Gabor patch increases linearly with increase in speed of the grating of the Gabor patch and the duration of presentation. Movie S4 is a circular path of Gabor patches with the speed of the centrifugal motion modulated around the path. Over time, the pattern is seen to assume a rounded triangle shape evocative of the shape of a spatial RF pattern. Figure 6 shows the thresholds for the amplitude of centrifugal speed modulation around otherwise circular paths. Thresholds are plotted against number of cycles of modulation and are fitted with power functions.

A two-tailed, paired-samples *t*-test comparing the indices of the power functions for the psychometric data with those for the probability summation predictions showed that the rate of decrease of the thresholds with increasing numbers of cycles of modulation exceeded that predicted by probability summation ($t(4) = 3.413$, $p = 0.0270$, $BF_{10} = 3.451$). This result implies an integration of information around the pattern.

Dickinson, Han, et al. (2010) showed that the perceived displacement of a Gabor patch due to De Valois effect could be as much as 90% of the extrapolated position of its contained moving grating over the duration of stimulus presentation. Assuming such an extrapolation of position, a threshold amplitude of speed modulation of 0.3 for a single cycle of modulation equates to a displacement of 0.065 degrees of visual angle over the 480 ms stimulus presentation, or an amplitude of positional modulation of 0.03 for patterns with a radius of 2.25 degrees. This is the threshold amplitude measured for positional modulation in Experiment 2. In order to visualize how the position, orientation, and motion modulation information is integrated within a cycle of modulation and then how the information is integrated across cycles of modulation a final, critical experiment, Experiment 4, was performed.

Experiment 4: Thresholds for modulation of position, orientation and centrifugal speed in RF patterns are consistent with sensitivity to positional modulation incorporating the twisted cord illusion and the De Valois effect

In this experiment, the applied amplitudes of modulation of position, orientation, and motion were normalized, to match the salience of each cue, using the ratio between the thresholds for a single cycle of modulation of position and speed and the threshold

Downloaded from hwmaint.iovs.org on 04/25/2024

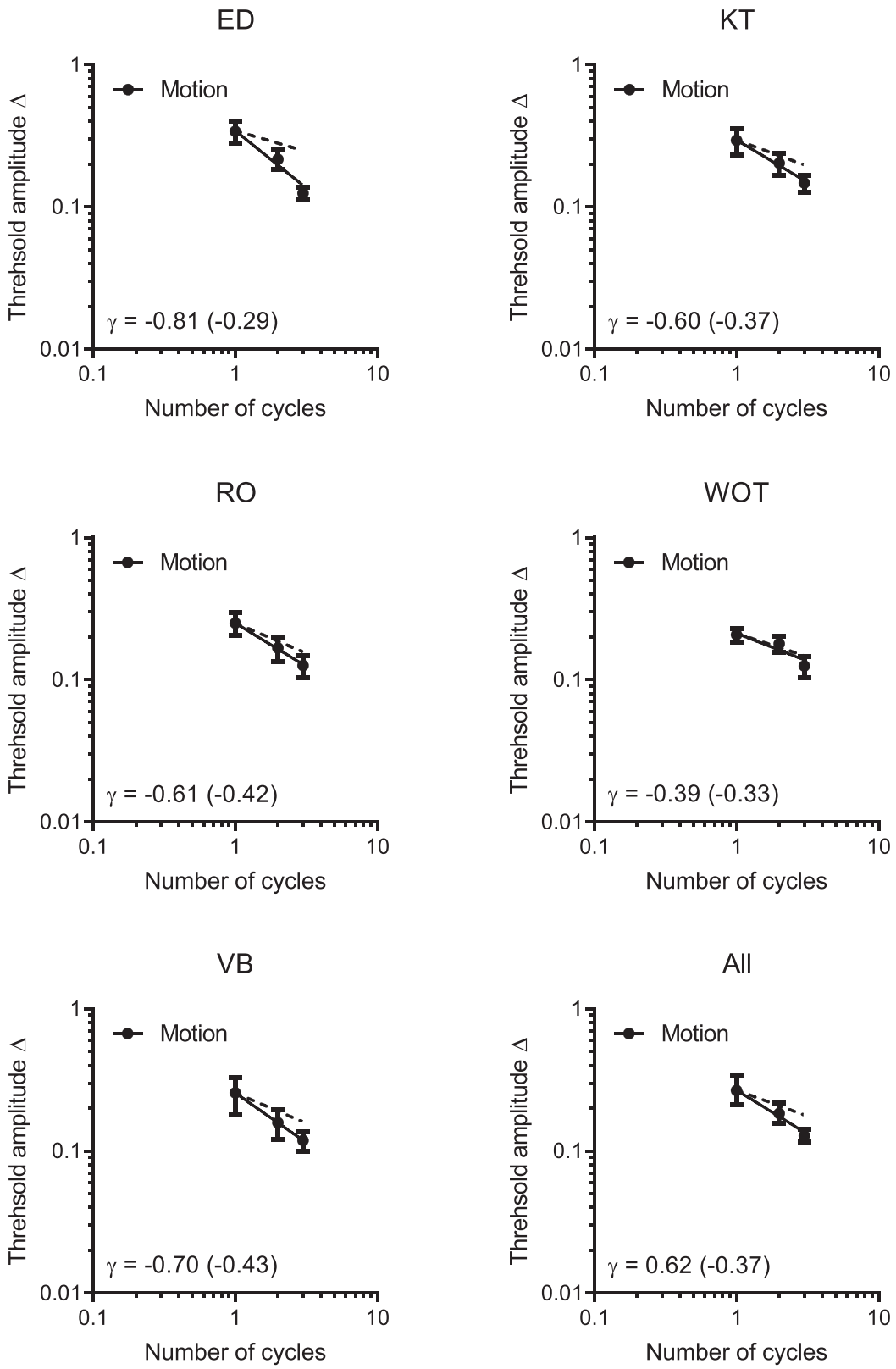

Figure 6. Thresholds for detection of modulation of centrifugal speed. Thresholds are plotted against number of cycles of sinusoidal modulation of centrifugal speed. Error bars represent 95% confidence intervals and the solid black lines are fitted power functions. The dashed black lines represent probability summation predictions. The indices of the power functions describing the data are reported in each panel along with, in brackets, those describing the probability summation predictions.

Downloaded from hwmaint.iovs.org on 04/25/2024

for a single cycle of orientation modulation. This was done to ensure we could produce equally detectable amounts of modulation of each cue type on a single cycle. We have shown that position and orientation modulation are approximately equally salient and that adding orientation modulation to position modulation halves the threshold, implying linearity in the signal strengths of these cues with amplitude of modulation. For each observer, ratios between single cycle thresholds of position and orientation modulation, and speed and orientation modulation were determined. This allowed position, orientation, and speed modulation to be added to the patterns as orientation modulation equivalents. The three different types of modulation could then be added as unitary cues and we might expect the threshold amount of each single cue to decrease as cues are added. For example, a single cycle of positional modulation might be added to a pattern, followed by orientation and then speed modulation, with all amplitudes of modulation added as their orientation modulation equivalents. One, two, and three cues are added under these circumstances and the orientation equivalent threshold amplitude can be plotted against the number of cues. This process was extrapolated to the second and third cycles of the RF3 patterns by adding position, orientation, and speed modulation to the second and then the third cycles, deriving orientation equivalent threshold amplitudes for six and nine cues. The analysis was performed in this manner so that the summation of different cues on one cycle and the combined cues across cycles could be compared. If these were substantially different, then this would be evident as a dog-leg in the power function at three cues. Thresholds, normalized to those seen for orientation modulation, are plotted in Figure 7 against the number of cues present.

Power functions are fitted to the data displayed in Figure 7 and are seen to represent the data well over the full range of number of cues present. Probability summation predictions for the indices of the power functions expected if the individual cues were detected independently were calculated using the SDT method described earlier but also including threshold predictions for six and nine cues present. A two-tailed, paired-samples *t*-test comparing the indices of the power functions fitted to the psychometric data with those of the power functions fitted to the probability summation predictions for thresholds for one, two, three, six, and nine cues showed that the rate of decrease of the thresholds with increasing numbers of cycles of modulation differed from that predicted by probability summation ($t(4) = 4.461$, $p = 0.011$, $BF_{10} = 6.514$).

Discussion

In this study, we have shown that a perceived modulation in a circular path of Gabor patches can be induced by physically modulating the positions of the patches radially, modulating their orientation as though they were aligned with a modulated path, and by modulating the centrifugal speed in the gratings of the Gabor patches.

In Experiment 1, we demonstrated that thresholds for detection of a sinusoidal modulation of radius in the path of Gabor patches is neither impaired, nor enhanced, when a constant centrifugal speed is introduced to the gratings of the Gabor patches. This result is in accordance with the demonstration, using an adaptation paradigm, of an insensitivity of the analysis of curvature to global motion implied by the motion of the carrier gratings of Gabor patches making up a sinusoidally modulated path (Gheorghiu, Kingdom, & Varshney, 2010). Global motion of the adaptor itself, however, does impact curvature adaptation (Gheorghiu & Kingdom, 2017; Gheorghiu et al., 2010). Modulation of the speed of the gratings also results in the phases of adjacent patches changing over time. Given that it has been shown that polarity reversal, particularly at points of maximum curvature, can result in decreased sensitivity to curvature features (Bell, Gheorghiu, Hess, & Kingdom, 2011) and a reduction in the increase in the salience of a boundary afforded by closure (Elder & Zucker, 1993; Schira & Spehar, 2011) it is important for the purposes of our study that the local motion has no effect on thresholds for detection of positional modulation. The phases of the gratings of the Gabor patches are initiated at random and, therefore, the chance alignment of the phases of the gratings of adjacent patches occurs at random across all of our stimulus classes. The results of Experiment 1 lend confidence to the assumption that the shape of the patterns is defined by the envelope of the path of Gabor patches and that the envelope is always perceived as closed.

Day and Loffler (2009) argued for independent global mechanisms for the analysis of position and orientation modulation around spatial RF patterns. On that basis, they would ascribe the percept of shape evident in the second and third patterns of Figure 2 of this paper to different mechanisms, with the most reliable interpretation of shape prevailing. However, in Experiment 2 of this study, we showed that the effects of modulation of position and orientation are additive. That is, the threshold for detection of modulation in a pattern that has position and orientation modulation is half that for patterns with solely position or orientation modulation. We believe the most parsimonious explanation for the decrease in threshold as orientation is added to position modulation is a release from the twisted cord illusion that operates in the opposite sense to the positional modulation when present in isolation. When the orientation modulation is present alone, the twisted cord illusion causes an illusory positional modulation of the same sign as the nominal RF modulation from which the orientations are

Downloaded from hwmaint.iovs.org on 04/25/2024

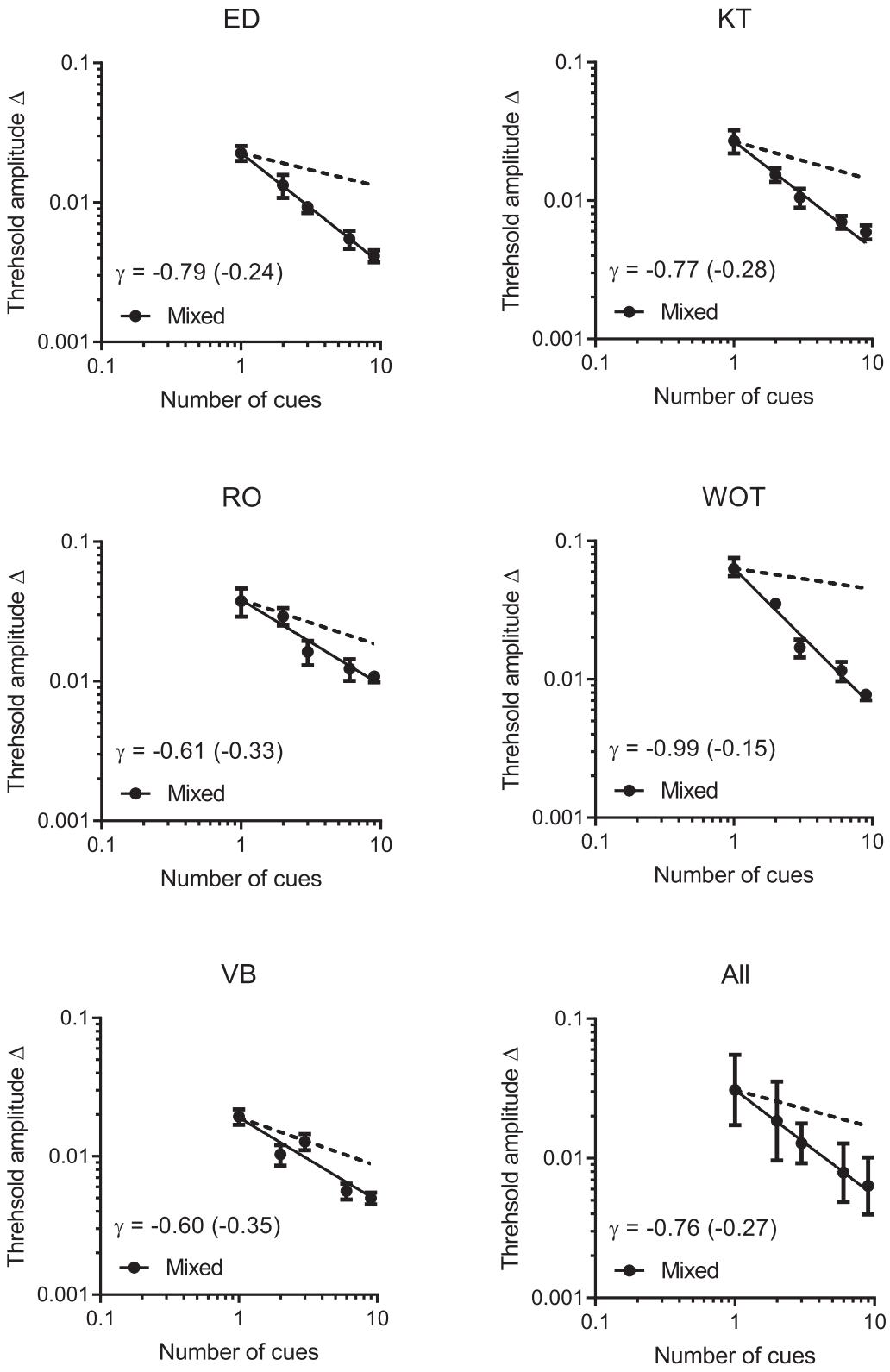

Figure 7. Thresholds for detection of modulation of position, orientation and centrifugal speed when combined within and across cycles of modulation. The quantity on the x-axis is the number of individual cues on a pattern with each cue normalized in salience. The cues were added incrementally, in different orders, to the first cycle of modulation across observers. It is evident from the data for each observer that the order in which the cues are added is unimportant, validating the normalization process. The data points at three, six, and nine cues had all three cues combined on one, two and three cycles of modulation respectively. The threshold amplitude is expressed as equivalent orientation modulation. Error bars represent 95% confidence intervals and the solid black lines are fitted power functions. The dashed black lines represent probability summation predictions.

Downloaded from hwmaint.iovs.org on 04/25/2024

Figure 8. Phase dependence of a combination of position and orientation modulation. The pattern on the left has positional (but no orientation) modulation with an amplitude of 0.05, approximately five times detection threshold. The central pattern has orientation (but no positional) modulation, also with an amplitude of 0.05, but in the opposite phase. The pattern on the right has both position and orientation modulation of amplitude 0.05, but in opposite phases, and appears substantially more circular.

drawn. Adding the positional modulation abolishes the twisted cord illusion, as the patches are now aligned along the path, and reduces the threshold. A strong prediction of this postulate is that the addition of the position and orientation modulation would be dependent on the relative phases of the position and orientation modulation. If the position and orientation modulation were in opposite phases, then the effect of the twisted cord illusion would be in opposition to the position modulation. Figure 8 illustrates that when they are in opposite phases the position and orientation modulation can cancel.

That the pattern on the right in Figure 8 appears circular illustrates the phase sensitive interaction between the position and orientation modulation and demonstrates that the suggestion of Day and Loffler (2009), that independent mechanisms analyze position and orientation modulation, and that the percept of shape is determined by the most reliable information, can be rejected (if the information were equally reliable then it might be argued that a bi-stable percept would result, but there is no evidence for this in Figure 8). Rather, we argue that the positions of the Gabor patches are modified in perception to accommodate the twisted cord illusion introduced into the envelope of the path of Gabor patches locally, in order to preserve path continuity. The result seen in the right-hand pattern of Figure 8 is that a path that is physically modulated in position can be perceived as circular.

Experiment 3 demonstrated integration of information around a circular path of Gabor patches whose carrier gratings had a sinusoidally modulated centrifugal speed. We conclude that local illusory positional displacements that are proportional to the local amplitude of speed modulation result in a path that is perceived as having positional modulation. The sinusoidal modulation of centrifugal speed leads to a perceived sinusoidal modulation of position through the De Valois effect expressed locally in each Gabor patch. Of course, if the orientation of the Gabor patches remains constant throughout the stimulus presentation, then the patches will remain oriented as though they are tangent to a circle. The apparent sinusoidal modulation of radius will, therefore, result in a twisted cord illusion in opposition of the modulation induced by the De Valois effect.

Experiment 4 showed that successively adding positional, orientation, and centrifugal speed cues, of normalized salience, reduced the threshold for detection at a rate that could not be accounted for by probability summation. Although the three types of cue were normalized for salience, they do not map directly onto the twisted cord and De Valois illusions. For example, adding positional modulation in the absence of modulation of orientation and centrifugal speed actually introduces positional modulation along with an opposing twisted cord illusion. Subsequently adding orientation modulation of the same amplitude in the same phase aligns the axes of the Gabor patches in the modulated path, thereby removing the twisted cord illusion. Adding centrifugal speed modulation results in an increase in perceived amplitude but reintroduces an opposing twisted cord illusion. Given that a single power function fits the threshold data as the three cues are added to a single cycle, and then additional cycles containing all three cues are added, suggests a linearity of size of the twisted cord illusion and DeValois effect with positional modulation and modulation of centrifugal speed respectively, as we have previously shown (Dickinson, Han, et al., 2010; Dickinson, Harman, et al., 2012). Experiment 4, therefore, demonstrates that the effect of the twisted cord illusion and the De Valois effect are additive and that they add to genuine modulation of position.

Although it is the case that modulating orientation from tangential to a path introduces the twisted cord illusion acting in the opposite sense, Figure 9 shows that it is possible to add a twisted cord illusion to a pattern modulated in position and orientation (and therefore not subject to the twisted cord illusion) which acts in the same sense. The figure also provides a static illustration of addition of the De Valois effect to a pattern that is modulated in position and subject to the twisted cord illusion.

The conclusions we draw from this study is that independent illusions, such as the twisted cord illusion and De Valois effect, are additive, and that shape perception, like the earlier binding of contours (Hayes, 2000), uses the apparent positions of the boundaries of objects in its analysis rather than their veridical positions. The implications of these conclusions for the interpretation of data pertaining to the visual analysis of shape are profound. Rather than requiring multiple parallel mechanisms for the interpretation of the spatial form of position, orientation, and radial

Downloaded from hwmaint.iovs.org on 04/25/2024

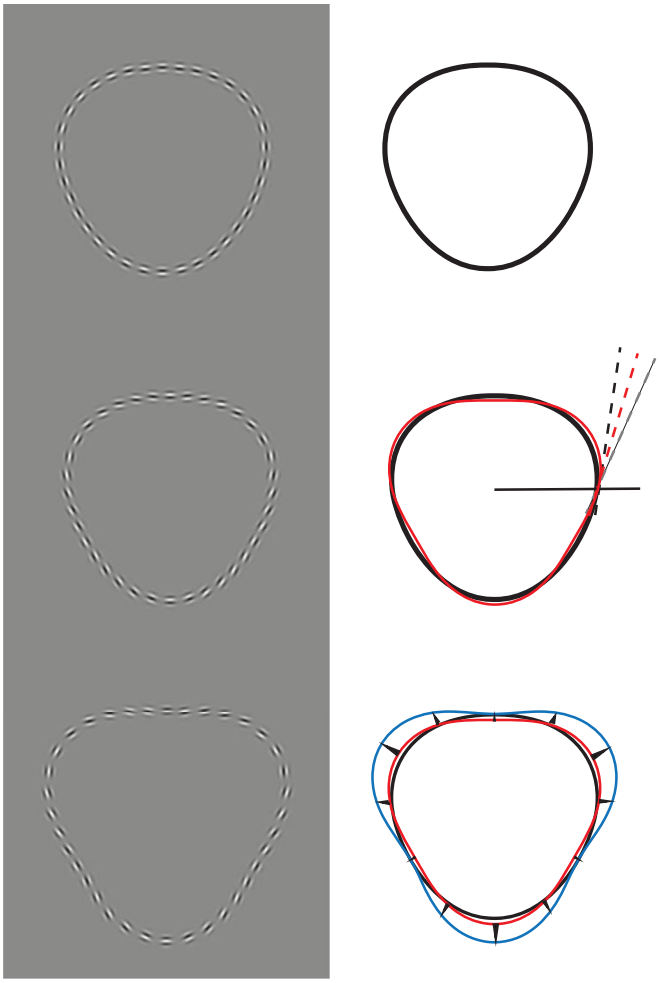

Figure 9. An illustration of the addition of the twisted cord illusion and then the De Valois effect to a path of Gabor patches sinusoidally modulated in radius. In the top row the radius of a path of Gabor patches is modulated with an amplitude of 0.05. The patches of the path also have a modulation of orientation in the same phase with an amplitude of 0.05 and, therefore, the axes of the patches are aligned tangential to the path. Consequently, the twisted cord illusion is absent. The path described by the black line has the same amplitude of modulation and appears to have the same shape. In the second row, the amplitude of modulation of radius is the same as in the top row, at 0.05, but the amplitude of orientation modulation is 0.15, thereby introducing a twisted cord illusion. The pattern appears to have a larger amplitude of modulation, it appears even less like a circle. A red line pattern with an amplitude of 0.1 is added to the illustration to the right, which appears to have a similar amplitude of modulation as the Gabor sampled path. A solid black line projects from the center of the pattern and intersects the pattern as a point where the amplitude of modulation is zero. At this point, patterns with a modest amplitude of modulation deviate maximally in orientation from circular. A dashed black line is tangent to the physical path (bold black line) at this point. The dashed grey line is aligned along the axis of the Gabor patch at this point and, for modest amounts of modulation, this is where the patch orientation

→

speed, it appears that the processing of shape can be constrained to a single mechanism responsible for the analysis of the form of a contour that incorporates local illusions of position that might be structured if such local illusions have a degree of coherence. The De Valois and twisted cord illusions might arise from the contour binding imperative of the visual system with the illusory positional displacement of the De Valois effect a consequence of a mechanism to compensate for delays intrinsic to processing of visual information through predicting the future position of a contour in motion (Nijhawan, 1994). The dependence of the De Valois effect on time and speed demonstrated by Dickinson, Han, et al. (2010) and others (Arnold, Thompson, & Johnston, 2007; Chung, Patel, Bedell, & Yilmaz, 2007) would then reflect what would be a necessary property of such a mechanism for predicting position. Interestingly, McGraw, Whitaker, Skillen, and Chung (2002) demonstrated that the position of a static Gabor patch was misperceived, post adaptation to a Gabor patch with a moving carrier grating, even when the grating of the test patch was orthogonal to that of the adapting patch, a condition where no motion aftereffect would be expected. This result is consistent with a general local displacement, in the direction of motion, of the perceived position of the next feature presented at the point previously occupied by the

←

deviates maximally from the orientation of the path. The dashed red line is tangential to the red path representing the perceived shape of the path of Gabor patches. The three dashed lines illustrate that the orientation of the perceived path is drawn towards the orientation of the Gabor patch. The bottom row illustrates the addition of a modulation of centrifugal speed to the pattern. In the absence of motion, for this static illustration, an additional amplitude of modulation of 0.05 has been added to the modulation of the physical path in lieu of the De Valois illusion. As the size of the De Valois effect is a linear function of the speed of the gratings of the patches (Dickinson, Han, et al., 2010), the illusory modulation is sinusoidal. The mean radius of the path has also been increased by one eighth to illustrate the illusory expansion of the stimulus due to the background centrifugal speed of the patches. An additional amplitude of orientation modulation of 0.05 has been added so that the twisted cord illusion is not added to when making this transformation. In a genuine motion stimulus, because the modulation due to the De Valois effect grows over time, this orientation modulation would need to be added incrementally to prevent a change in the twisted cord illusion over time. The perceived shape is illustrated in blue with the illusory displacement of the path from the red path to the blue denoted by arrows. The total illusory displacement due to the combined effect of the twisted cord illusion and the De Valois effect is the difference between the black and the blue paths.

Downloaded from hwmaint.iovs.org on 04/25/2024

windowed carrier grating. A continuously presented Gabor patch with a moving carrier grating might be expected to migrate in the direction of motion, as is seen.

Similarly, the twisted cord illusion could arise from a mechanism responsible for binding paths on different spatial scales. Dickinson, Harman, et al. (2012) have previously proposed a model to account for the twisted cord illusion based on the encoding of orientation within a bank of channels which are individually sensitive to a range of orientations and collectively cover the whole range of orientations. Orientation selective neurons of the primary visual cortex are too broadly tuned for orientation to account for human performance in discriminating between orientations and so, here, we adopt the model of Dickinson, Harman, et al. (2012) and propose that perceived orientation is encoded in a population of neurons that collectively comprise a bank of orientation selective channels spanning the full range of possible orientation. Specifically, orientation is encoded in the direction of a sum of vectors representing the activity in each of the channels. The length of each vector represents the magnitude of response of each channel to the oriented stimulus, with the vector direction representing the preferred orientation of each channel in a double angle space (Clifford, Wenderoth, & Spehar, 2000). The double angle space allows for a vectorial representation of orientation where vectors pointing in opposite directions represent orthogonal orientations. The model was adapted from that proposed to account for reaching directions in 3D space and instantiated in the primary motor cortex (Georgopoulos, Kettner, & Schwartz, 1988; Georgopoulos, Schwartz, & Kettner, 1986) but collapsed from 3D space onto the 2D space necessary to define orientations uniquely in the visual field (Gilbert & Wiesel, 1990; Vogels, 1990). To account for the twisted cord illusion, an excitatory gain connection is postulated between orientation selective channels in discrete banks with the same orientation preference but different spatial scales. The twist in the cord stimulates channels sensitive to orientation information on a smaller spatial scale, which then enhance the sensitivity of channels with the same orientation preference but of a larger spatial scale appropriate for detection of the envelope of the cord itself. The local orientation of the cord is then misperceived in the direction of the twist of the cord. If the excitatory gain enhancement in the channels of one bank is in proportion to the degree to which the channels of the other is stimulated, then the function that predicts the twisted cord illusion across the whole range of orientation difference between the twist in the cord and the axis of the cord matches that which is observed (Dickinson, Harman, et al., 2012). Such a mechanism would serve to enhance similar orientation signals extant at different spatial scales. The propagation of a path incorporating a misperception of its local orientation results in a misperception of position. Figure 10 illustrates the proposed model of orientation encoding that predicts the local twisted cord illusion.

It is intriguing that such disparate phenomena as the twisted cord illusion and the De Valois effect can lead to the same misrepresentation of shape. We will, therefore, speculate on a possible common principal that might underlie the two effects. It is reasonable to assume that the neuronal receptive fields of the primary visual cortex, the level in the visual processing hierarchy that is characterized by orientation selectivity, maps onto the visual field in a reasonably stable manner. However, local features of the visual field are systematically misperceived in position. One way in which the misperception of position might occur is through lateral excitatory connections between neurons with overlapping but displaced receptive fields.

For the twisted cord illusion, we have argued above that the orientation of a local section of the cord is misperceived to be more similar in orientation to the twist in the cord than it actually is. The orientations of both the twist in the cord and the cord itself are both perceived and we will assume that the orientations of the Gabor patches are encoded by first-order, luminance properties and that the local orientation of the cord is encoded by second-order texture or contrast properties. It has previously been shown that the salience of sampled paths in noise is enhanced by collinearity of adjacent elements (Field, Hayes, & Hess, 1993; Li & Gilbert, 2002), and it has been proposed that this is due to lateral excitatory connections between neurons with collinear receptive fields. Increased sensitivity of neuronal receptive fields centered on a projected path might cause stimuli adjacent to the path to be perceived as nearer the path than they actually are, lending the path some perceptual stiffness and making position somewhat subordinate to continuity of the path. Previously we have used Euler's method to predict the perceived shapes of paths subject to local contextual illusions (Bowden et al., 2019; Dickinson, Almeida, et al., 2010; Dickinson, Harman, et al., 2012). Obviously, the visual system would not use a serial system of determining the form of a path but it is conceivable that excitatory connections between neurons signaling illusory orientations will result in the perceived position of the path being displaced, due to the enhancement in sensitivity of receptive fields that are not centered on the physical path, if the local position is encoded in the responses of a population of neurons. The distance over which position can be misrepresented is, therefore, constrained by the extent of the receptive fields. Figure 11 illustrates a potential mechanism.

Considering the De Valois effect, if neurons with receptive fields in the direction of motion were enhanced in sensitivity, and the stimulus position encoded in the centroid of the stimulated population of

Downloaded from hwmaint.iovs.org on 04/25/2024

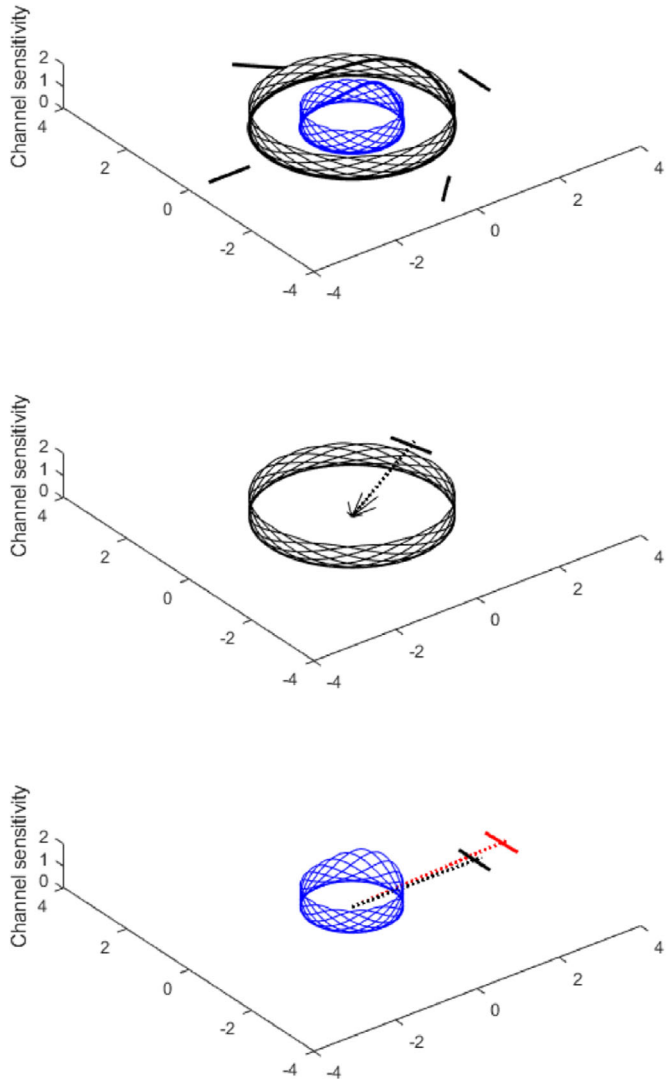

Figure 10. A model of orientation encoding that predicts the twisted cord illusion. The top panel depicts two banks of orientation selective channels spanning the full range of possible orientations in a double angle space. The preferred orientations of the channels are illustrated by the black bars external to the banks of channels. The channels depicted in black are assumed to be sensitive at the spatial scale of the twist in the cord. Those in blue are assumed to be sensitive to the spatial scale of the envelope of the cord. It is proposed that excitatory connections exist between channels with the same orientation preference across these two banks of channels. Example channels with the same orientation preference are shown in bold. The middle panel illustrates the response to a twist in the cord of 15 degrees to the vertical. The fan of black lines radiating from the center are vectors representing the responses of the channels to the twist in the cord. The length of each vector is the channel response, and each vector points in the direction of its preferred orientation. The vector sum (dashed black line) represents the perceived orientation of the twist in the cord. The sensitivities of the channels illustrated in the bottom panel have been modified by the excitatory connections between channels with similar orientation

→

neurons, then the perceived position would be displaced in the direction of motion. Such an effect might be expected to propagate in the direction of motion, with the enhanced response of a neuron with a receptive field offset in the direction of motion providing excitatory input to the next, and so on. The range of the effect would, of course, be constrained by the extent of the receptive fields. An illustration of this potential mechanism is shown in Figure 12.

The mechanisms proposed above are speculative but they would potentially allow the illusions to be supported mechanistically within the primary visual cortex and so the illusions would naturally propagate through the hierarchy of retinotopic visual areas without the necessity for remapping of neuronal connectivity between such areas, and without requiring feedback. Misperception of position arises from a population encoding, which is biased by lateral excitatory connections between neurons with overlapping/adjacent receptive fields.

Obviously, it is difficult to know conclusively that the visual system assembles a path incorporating local contextual illusions, the conformation of which becomes the basis for the analysis of shape, but the pattern on the right of Figure 8 illustrates that patterns that contain modulation of position and orientation can appear circular. Similarly, modulation of centripetal speed can abolish the perception of shape in a pattern modulated in position if the modulation is applied in the opposite phase.

Stating that shape is absent when the pattern appears circular casts the circle as a null or prototypical shape but we do not do this without some evidence. In visual search experiments, we have shown that spatial RF patterns are easily identified among circles but circles are difficult to find among RF patterns (Dickinson, Haley, Bowden, & Badcock, 2018), implying that the RF patterns contain a cue that the circles do not, and

←

preferences across the two banks of channels. The sensitivities of the channels that are sensitive to the orientation of the cord are enhanced in proportion to the response of channels sensitive to the twist in the cord. The twist in the cord biases the population response of the bank of channels sensitive to the envelope of the cord, causing its orientation to be misperceived in the direction of the twist in the cord. The perceived orientation of a vertical cord in the absence of a twist in the cord is shown by the dashed black line and the predicted perceived orientation for a cord with a 15 degree twist is shown by the dashed red line (the maximum enhancement in sensitivity was set arbitrarily, for this illustration, to be 50%). The orientation is shown to be displaced towards the twist in the cord (the red dashed line is anti-clockwise of the black dashed line).

Downloaded from hwmaint.iovs.org on 04/25/2024

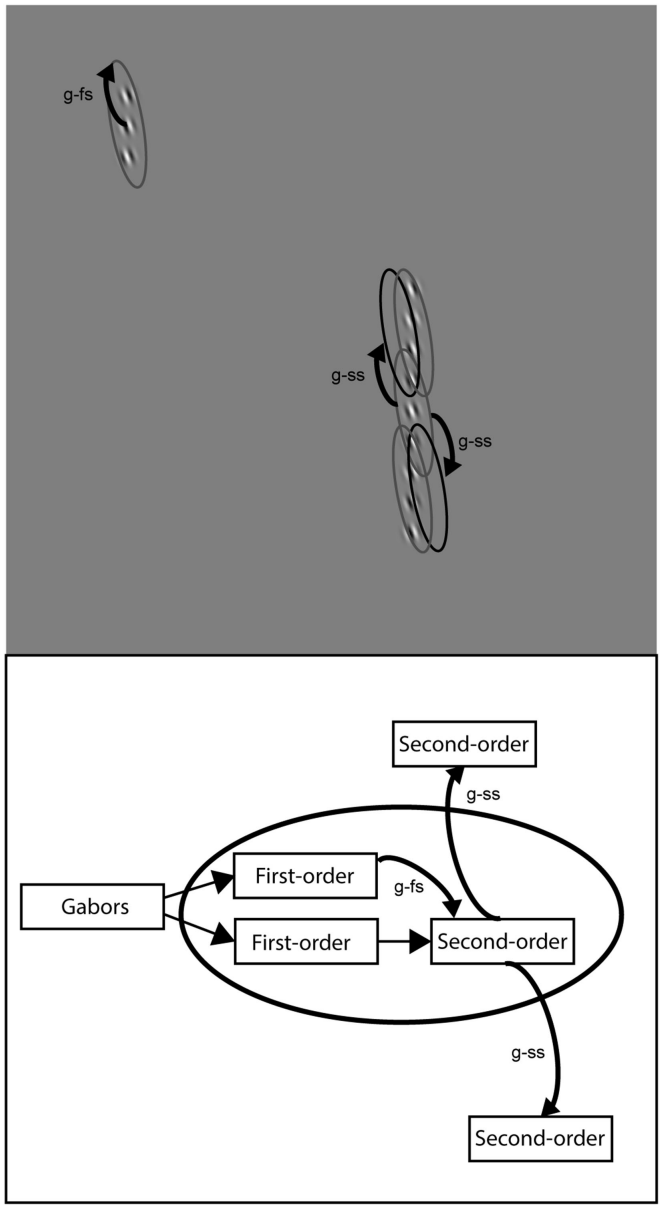

Figure 11. An illustration of the mechanism proposed to account for the perceived displacement of a path of Gabor patches due to the local twisted cord illusion. The mechanism assumes excitatory gain connections (g-fs) between distinct banks of orientation selective channels sensitive to the orientation of the patches (first-order, f) and the orientation of the path (second-order, s). Top left is an illustration of the local twisted cord illusion with the perceived orientation of the path of patches (ellipse) misperceived as drawn towards the orientation of the axes of the Gabor patches. The mechanism proposed to support this illusion is described above and illustrated in Figure 10. In the flow diagram it is represented within the ellipse. It is then proposed that the misperception of the local position of the path is supported by excitatory lateral connections (g-ss) between neurons with adjacent and collinear second-order receptive fields.

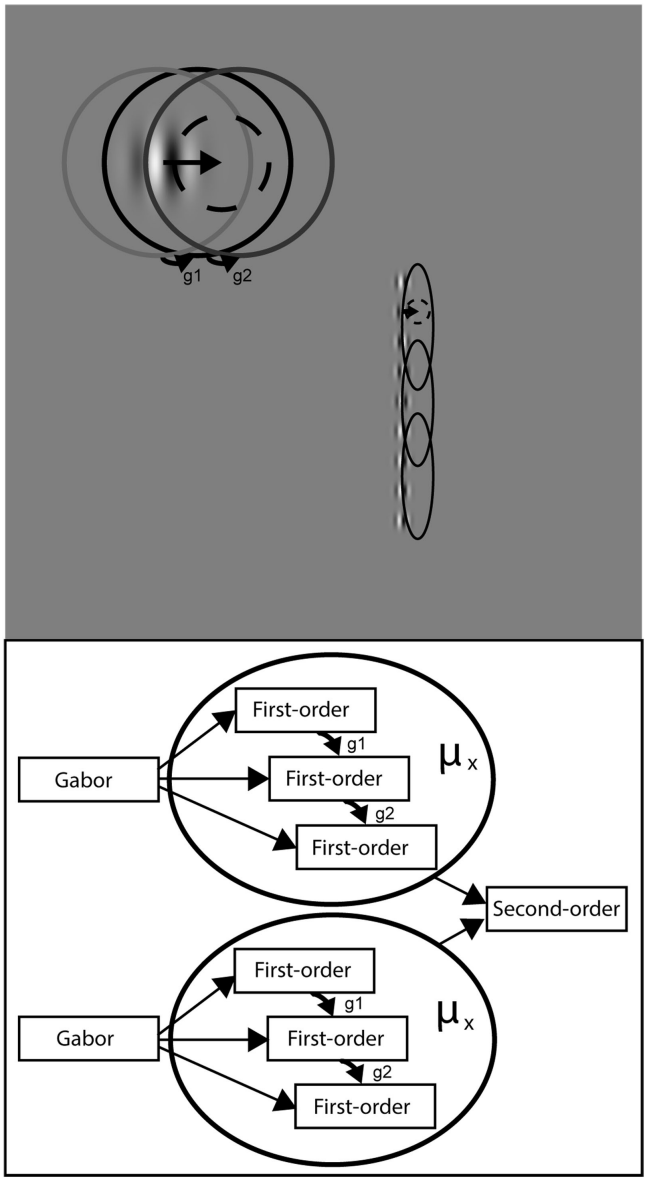

Figure 12. An illustration of the mechanism proposed to account for the perceived displacement of a path due to the local De Valois effect. The circles overlapping the Gabor patch top-left represent motion selective receptive fields. Excitatory connections are proposed between neurons with similar motion direction preference (g1 and g2) but only in the direction of motion. This has the effect of increasing sensitivity in the direction of motion. If position is then encoded in the population response of the motion selective neurons (μ_x), then the patch would be perceived as displaced in position in the direction of motion (dashed circle). Further, if a path of patches is moving coherently then the second-order envelope of the path would be perceived as displaced in position in the direction of motion of the gratings of the patches. The potential mechanism of the De Valois effect is contained by the ellipses in the flow diagram.

Downloaded from hwmaint.iovs.org on 04/25/2024

that the converse is not true (Treisman & Gelade, 1980; Treisman & Souther, 1985). Although it would be easy to assume that the cue is provided by a global analysis of the sinusoidal modulation of the path from circular and, by extension, that compound RF patterns might represent more complex shapes, it has always been clear that many articulated shapes, for example, animal bodies, cannot be represented solely as a single compound of RF patterns of differing frequency, amplitude, and phase (Schmidtmann & Fruend, 2019). Indeed, it is easily appreciated that the boundaries of many complex shapes can intersect the same radius from the object center more than once. The recognition by components theory (Biederman, 1987) proposes that complex objects are dissociated at matched concavities on their boundaries into simpler shapes with no more than one concavity. Such patterns might lend themselves to analysis in terms of radial basis functions, but much more work needs to be done to demonstrate that this is a plausible model. We prefer a model based on the relative polar positions of points of maximum curvature on the path with respect to the pattern center.

Neurophysiological studies have shown that single neurons of cortical area V4 are sensitive to local curvature features, in particular orientations (Pasupathy & Connor, 1999), and it has been proposed that populations of such neurons might encode shape in a 2D parameter space of polar angle by curvature, with respect to the center of the pattern (Pasupathy & Connor, 2001; 2002). A biologically inspired model proposed to account for psychophysical data uses measures of local curvature to identify points of maximum convex curvature in the analysis of shape, rather than a decomposition into RF components (Poirier & Wilson, 2006). More recent neurophysiological studies have suggested that the distribution of curvature selectivity of neurons of V4 is weighted towards points of high curvature (Carlson, Rasquinha, Zhang, & Connor, 2011). This implies that simple shapes might be encoded in an economic manner by the positions of points of maximum convex curvature relative to the pattern centers, with complex shapes decomposed at matched concavities (Biederman, 1987; Wong, Dickinson, & Badcock, 2020). Dickinson et al. (2018) also showed in their visual search study that patterns with three cycles of negatively rectified sinusoidal modulation of radius were hard to identify among conventional RF patterns with three cycles of modulation and vice versa. These patterns have different distributions of absolute curvature but identical distributions of points of maximum curvature (see also Dickinson, Cribb, Riddell, & Badcock 2015). This result provides corroborating evidence that it is the configuration of points of maximum curvature that discriminate such patterns, rather than an analysis of absolute curvature around the patterns. Such an encoding of shape might be expected to be relatively robust to the effects of local positional illusions on the conformation of a path.

The misperception of the locus of the path is required to preserve the continuity of the path of Gabor patches in the presence of local misperception of orientation of the path due to the twisted cord illusion. The twisted cord illusion is well represented by a first derivative of a Gaussian (D1) function of that orientation difference, which peaks at an orientation difference of around 20 degrees to 30 degrees (Dickinson, Harman, et al., 2012). The size of the local illusion, therefore, increases approximately linearly for differences up to 15 degrees to 20 degrees. Consequently, a sinusoidal modulation of orientation not exceeding such angular differences produces a sinusoidal modulation in the magnitude of the illusion and, if the continuity of the path is preserved at the expense of accuracy in the perceived position of the path, a sinusoidal modulation in illusory amplitude of positional modulation. Sensitivity to the shapes of RF patterns is commonly quoted as threshold amplitudes of modulation. We have, however, previously shown that the property of an RF pattern that is equated at the threshold modulation amplitude across patterns with the same number of cycles of modulation but differing frequencies of modulation is the maximum angular deviation from circular (Dickinson, McGinty, et al., 2012). This property is also equated across patterns with sinusoidal and rectified sinusoidal modulation of radius but the same period of points of maximum curvature (Dickinson et al., 2015). Across such pattern types, local curvature can vary significantly and so it would seem extremely unlikely that a single family of radial basis function could be used to decompose disparate shapes. Rather than decomposition, our preferred model relies on an encoding of the positions of points of maximum curvature relative to the pattern center. It is proposed that the positions of such points, rather than being derived from continuous measures of curvature, might be identified by corner detectors indifferent to the absolute measure of the curvature. A representation of shape in the form of an ordered set of such angles would be scale and rotation invariant. We would concede, however, that much of this is conjecture and more work will be required before the mechanism by which shape is encoded is finally established. In particular, such a simple encoding relies upon complex patterns being dissociated into component parts.

Although the results of this study are limited to threshold amplitudes of modulation of position, orientation, and centrifugal speed, which is an obvious limitation of the study, it is evident from Figures 2, 8, 9, and 10 that the twisted cord illusion can result in quite large amplitudes of apparent modulation. Similarly, Movie S4 shows that the De Valois effect can result in similarly large amplitudes of illusory spatial modulation. Future studies will seek to

Downloaded from hwmaint.iovs.org on 04/25/2024

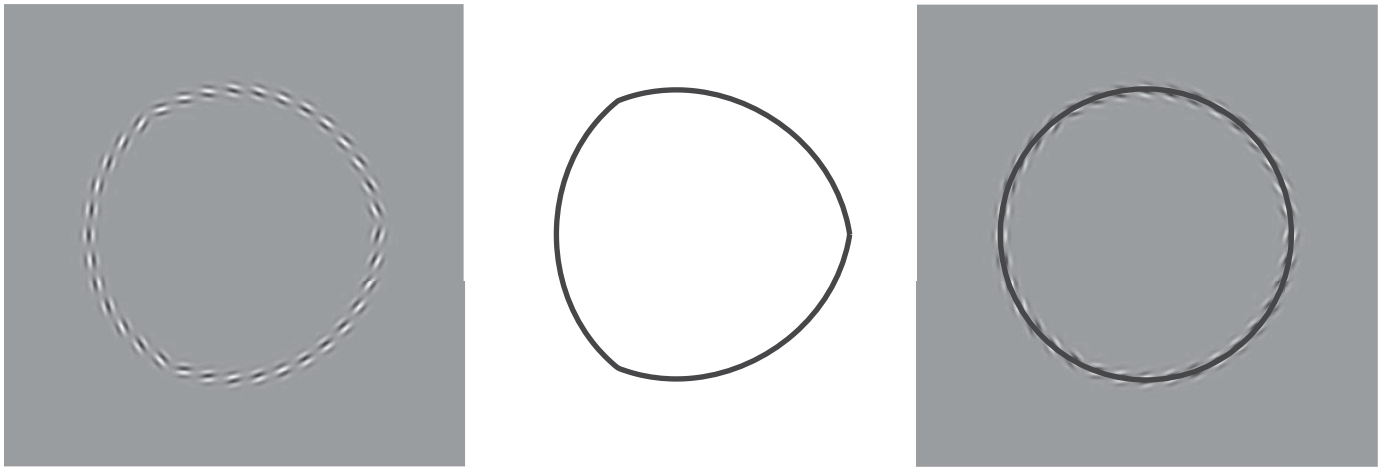

Figure 13. An illustration of the percept of shape due to a negatively rectified sinusoidal modulation of orientation in path of Gabor patches. On the left, the orientations of a circular path of Gabor patches equate to those of tangents to a path with a negatively rectified sinusoidal modulation of radius of 0.2. In the center, is a path with a negatively rectified sinusoidal modulation of radius of 0.1. The perceived shapes of the left and center patterns are similar. On the right a circle is superimposed on the pattern displayed on the left to demonstrate that it circular.

generalize the results presented here to supra-threshold shapes.

A second significant limitation of the study is that the shapes investigated are all RF patterns. This is the same limitation that may have led Day and Loffler (2009) to postulate a global detector for the sinusoidal modulation of orientation on a path and (Rainville & Wilson, 2004; Rainville & Wilson, 2005) a global detector for sinusoidal modulation of centrifugal speed, given that the twisted cord illusion and the De Valois effect magnitudes are linear with orientation difference from circular and speed respectively. Figure 13 illustrates the percept of shape produced by the twisted cord illusion in a circular path of Gabor patches whose orientations are subject to a negatively rectified sinusoidal modulation.

Figure 13 demonstrates that the illusion of shape conferred to closed paths is not restricted to RF patterns. We suggest, therefore, that the perceived local position of a path incorporates the twisted cord illusion and the De Valois effect and that the reconfiguration of the path precedes shape analysis.

Keywords: Fraser illusion, motion position illusion, shape, shape illusion

Acknowledgments

Supported by Australian Research Council Grants DP0666206, DP1097003, DP160104211, and DP190103474 to David R. Badcock.

Commercial relationships: none.
Corresponding author: J. Edwin Dickinson.
Email: edwin.dickinson@uwa.edu.au.
Address: School of Psychological Science, 35 Stirling Highway, University of Western Australia, Crawley, Perth 6009, Western Australia, Australia.

References

Arnold, D. H., Thompson, M., & Johnston, A. (2007). Motion and position coding. *Vision Research, 47*(18), 2403–2410.

Badcock, D. R., & Westheimer, G. (1985a). Spatial location and hyperacuity: flank position within the centre and surround zones. *Spatial Vision, 1*(1), 3–11.

Badcock, D. R., & Westheimer, G. (1985b). Spatial location and hyperacuity: The centre/surround localization contribution function has two substrates. *Vision Research, 25*(9), 1259–1267.

Baldwin, A. S., Schmidtmann, G., Kingdom, F. A. A., & Hess, R. F. (2016). Rejecting probability summation for radial frequency patterns, not so Quick! *Vision Research, 122*, 124–134.

Bell, J., Gheorghiu, E., Hess, R. F., & Kingdom, F. A. A. (2011). Global shape processing involves a hierarchy of integration stages. *Vision Research, 51*(15), 1760–1766.

Biederman, I. (1987). Recognition-by-Components: A Theory of Human Image Understanding. *Psychological Review, 94*(2), 115–147.

Biederman, I., & Ju, G. (1988). Surface versus edge-based determinants of visual recognition. *Cognitive Psychology, 20*(1), 38–64.

Downloaded from hwmaint.iovs.org on 04/25/2024

Bowden, V. K., Dickinson, J. E., Green, R. J., & Badcock, D. R. (2019). Phase specific shape aftereffects explained by the tilt aftereffect. *Journal of Experimental Psychology. Human Perception and Performance, 45*(7), 889–910.

Carlson, E. T., Rasquinha, R. J., Zhang, K., & Connor, C. E. (2011). A Sparse Object Coding Scheme in Area V4. *Current Biology : CB, 21*(4), 288–293.

Chung, S. T. L., Patel, S. S., Bedell, H. E., & Yilmaz, O. (2007). Spatial and temporal properties of the illusory motion-induced position shift for drifting stimuli. *Vision Research, 47*(2), 231–243.

Clifford, C. W. G., Wenderoth, P., & Spehar, B. (2000). A Functional Angle on Some After-Effects in Cortical Vision. *Proceedings: Biological Sciences, 267*(1454), 1705–1710.

Dakin, S. C., Williams, C. B., & Hess, R. F. (1999). The interaction of first- and second-order cues to orientation. *Vision Research, 39*(17), 2867–2884.

Day, M., & Loffler, G. (2009). The role of orientation and position in shape perception. *Journal of Vision, 9*(10), 1–17.

De Valois, R. L., & De Valois, K. K. (1991). Vernier acuity with stationary moving Gabors. *Vision Research, 31*(9), 1619–1626.

Dickinson, J. E., Almeida, R. A., Bell, J., & Badcock, D. R. (2010). Global shape aftereffects have a local substrate: A tilt aftereffect field. *Journal of Vision, 10*(13), 5.

Dickinson, J. E., & Badcock, D. R. (2007). Selectivity for coherence in polar orientation in human form vision. *Vision Research, 47*(24), 3078–3087.

Dickinson, J. E., & Badcock, D. R. (2013). On the hierarchical inheritance of aftereffects in the visual system. *Frontiers in Psychology, 4*, 472.

Dickinson, J. E., Cribb, S. J., Riddell, H., & Badcock, D. R. (2015). Tolerance for local and global differences in the integration of shape information. *Journal of Vision, 15*(3), 21.

Dickinson, J. E., Green, R. J., Harkin, G. M., Tang, M. F., & Badcock, D. R. (2019). A new visual illusion of aspect-ratio context. *Vision Research, 165*, 80–83.

Dickinson, J. E., Haley, K., Bowden, V. K., & Badcock, D. R. (2018). Visual search reveals a critical component to shape. *Journal of Vision, 18*(2), 2.

Dickinson, J. E., Han, L., Bell, J., & Badcock, D. R. (2010). Local motion effects on form in radial frequency patterns. *Journal of Vision, 10*(3), 1–15.

Dickinson, J. E., Harman, C., Tan, O., Almeida, R. A., & Badcock, D. R. (2012). Local contextual interactions can result in global shape misperception. *Journal of Vision, 12*(11), 3.

Dickinson, J. E., McGinty, J., Webster, K. E., & Badcock, D. R. (2012). Further evidence that local cues to shape in RF patterns are integrated globally. *Journal of Vision, 12*(12), 16.

Dickinson, J. E., Mighall, H. K., Almeida, R. A., Bell, J., & Badcock, D. R. (2012). Rapidly acquired shape and face aftereffects are retinotopic and local in origin. *Vision Research, 65*, 1–11.

Dickinson, J. E., Morgan, S. K., Tang, M. F., & Badcock, D. R. (2017). Separate banks of information channels encode size and aspect ratio. *Journal of Vision, 17*(3), 27.

Edwards, M., & Badcock, D. R. (2003). Motion distorts perceived depth. *Vision Research, 43*(17), 1799–1804.

Elder, J., & Zucker, S. W. (1993). The effect of contour closure on the rapid discrimination of two-dimensional shapes. *Vision Research, 33*(7), 981–991.

Field, D. J., Hayes, A., & Hess, R. F. (1993). Contour integration by the human visual system: Evidence for a local "association field". *Vision Research, 33*(2), 173–193.

Fraser, J. (1908). A new visual illusion of direction. *British Journal of Psychology, 1904-1920, 2*(3), 307–320.

Georgopoulos, A. P., Kettner, R. E., & Schwartz, A. B. (1988). Primate motor cortex and free arm movements to visual targets in three-dimensional space. II. Coding of the direction of movement by a neuronal population. *The Journal of Neuroscience, 8*(8), 2928–2937.

Georgopoulos, A. P., Schwartz, A. B., & Kettner, R. E. (1986). Neuronal population coding of movement direction. *Science, 233*(4771), 1416–1419.

Gheorghiu, E., & Kingdom, F. A. A. (2017). Dynamics of contextual modulation of perceived shape in human vision. *Scientific Reports, 7*(1), 1–15.

Gheorghiu, E., Kingdom, F. A. A., & Varshney, R. (2010). Curvature coding is tuned for motion direction. *Journal of Vision, 10*(3), 18–18.

Gilbert, C. D., & Wiesel, T. N. (1990). The influence of contextual stimuli on the orientation selectivity of cells in primary visual cortex of the cat. *Vision Research, 30*(11), 1689–1701.

Green, R. J., Dickinson, J. E., & Badcock, D. R. (2017). Global processing of random-phase radial frequency patterns but not modulated lines. *Journal of Vision, 17*(9), 18.

Green, R. J., Dickinson, J. E., & Badcock, D. R. (2018a). Convergent evidence for global processing of shape. *Journal of Vision, 18*(7), 7.

Downloaded from hwmaint.iovs.org on 04/25/2024

Green, R. J., Dickinson, J. E., & Badcock, D. R. (2018b). The effect of spatiotemporal displacement on the integration of shape information. *Journal of Vision, 18*(5), 4.

Green, R. J., Dickinson, J. E., & Badcock, D. R. (2018c). Integration of shape information occurs around closed contours but not across them. *Journal of Vision, 18*(5), 6.

Hayes, A. (2000). Apparent Position Governs Contour-Element Binding by the Visual System. *Proceedings: Biological Sciences, 267*(1450), 1341–1345.

Kourtzi, Z., & Kanwisher, N. (2000). Cortical Regions Involved in Perceiving Object Shape. *Journal of Neuroscience, 20*(9), 3310–3318.

Li, W., & Gilbert, C. D. (2002). Global Contour Saliency and Local Colinear Interactions. *Journal of Neurophysiology, 88*(5), 2846–2856.

Loffler, G., Wilson, H. R., & Wilkinson, F. (2003). Local and global contributions to shape discrimination. *Vision Research, 43*(5), 519–530.

Ly, A., Raj, A., Etz, A., Marsman, M., Gronau, Q. F., & Wagenmakers, E.-J. (2018). Bayesian reanalyses from summary statistics: A guide for academic consumers. *Advances in Methods and Practices in Psychological Science, 1*(3), 367–374.

McGraw, P. V., Whitaker, D., Skillen, J., & Chung, S. T. L. (2002). Motion Adaptation Distorts Perceived Visual Position. *Current Biology, 12*(23), 2042–2047.

Nijhawan, R. (1994). Motion extrapolation in catching. *Nature, 370*(6487), 256–257.

Pasupathy, A., & Connor, C. E. (1999). Responses to Contour Features in Macaque Area V4. *Journal of Neurophysiology, 82*(5), 2490–2502.

Pasupathy, A., & Connor, C. E. (2001). Shape Representation in Area V4: Position-Specific Tuning for Boundary Conformation. *Journal of Neurophysiology, 86*(5), 2505–2519.

Pasupathy, A., & Connor, C. E. (2002). Population coding of shape in area V4. *Nature Neuroscience, 5*(12), 1332–1338.

Poirier, F. J. A. M., & Wilson, H. R. (2006). A biologically plausible model of human radial frequency perception. *Vision Research, 46*(15), 2443–2455.

Prins, N., & Kingdom, F. A. A. (2018). Applying the Model-Comparison Approach to Test Specific Research Hypotheses in Psychophysical Research Using the Palamedes Toolbox. *Frontiers in Psychology, 9*, 1250.

Rainville, S. J. M., & Wilson, H. R. (2004). The influence of motion-defined form on the perception of spatially-defined form. *Vision Research, 44*(11), 1065–1077.

Rainville, S. J. M., & Wilson, H. R. (2005). Global shape coding for motion-defined radial-frequency contours. *Vision Research, 45*(25-26), 3189–3201.

Regan, D., & Hamstra, S. J. (1992). Shape discrimination and the judgement of perfect symmetry: Dissociation of shape from size. *Vision Research, 32*(10), 1845–1864.

Schira, M., & Spehar, B. (2011). Differential Effect of Contrast Polarity Reversals in Closed Squares and Open L-Junctions. *Frontiers in Psychology, 2*, 47.

Schmidtmann, G., & Fruend, I. (2019). Radial frequency patterns describe a small and perceptually distinct subset of all possible planar shapes. *Vision Research, 154*, 122–130.

Seu, L., & Ferrera, V. P. (2001). Detection thresholds for spiral Glass patterns. *Vision Research, 41*(28), 3785–3790.

Tan, K. W. S., Bowden, V. K., Dickinson, J. E., & Badcock, D. R. (2015). Modulated textures with shape structures implied by a closed flow are processed globally. *Journal of Vision, 15*(3), 17.

Tan, K. W. S., Dickinson, J. E., & Badcock, D. R. (2013). Detecting shape change: Characterizing the interaction between texture-defined and contour-defined borders. *Journal of Vision, 13*(14), 12.

Tan, K. W. S., Dickinson, J. E., & Badcock, D. R. (2016a). Discrete annular regions of texture contribute independently to the analysis of shape from texture. *Journal of Vision, 16*(11), 10.

Tan, K. W. S., Dickinson, J. E., & Badcock, D. R. (2016b). In unison: First-and second-order information combine for integration of shape information. *Journal of Vision, 16*(11), 9.

Tan, K. W. S., Scholes, C., Roach, N. W., Haris, E. M., & McGraw, P. V. (2021). Impact of microsaccades on visual shape processing. *Journal of Neurophysiology, 125*(2), 609–619.

Tang, M. F., Dickinson, J. E., Visser, T. A. W., & Badcock, D. R. (2015). The broad orientation dependence of the motion streak aftereffect reveals interactions between form and motion neurons. *Journal of Vision, 15*(13), 4.

Treisman, A. M., & Gelade, G. (1980). A feature-integration theory of attention. *Cognitive Psychology, 12*(1), 97–136.

Treisman, A. M., & Souther, J. (1985). Search asymmetry: a diagnostic for preattentive processing of separable features. *Journal of Experimental Psychology: General, 114*(3), 285.

Vogels, R. (1990). Population coding of stimulus orientation by striate cortical cells. *Biological Cybernetics, 64*(1), 25–31.

Downloaded from hwmaint.iovs.org on 04/25/2024

Webb, B. S., Roach, N. W., & Peirce, J. W. (2008). Masking exposes multiple global form mechanisms. *Journal of Vision, 8*(9), 1–10.

Wilkinson, F., Wilson, H. R., & Habak, C. (1998). Detection and recognition of radial frequency patterns. *Vision Research, 38*(22), 3555–3568.

Wilson, H. R. (1980). A transducer function for threshold and suprathreshold human vision. *Biological Cybernetics, 38*(3), 171–178.

Wong, V. S. Y., Dickinson, J. E., & Badcock, D. R. (2020). Shape partitioning interacts with global shape integration. *Vision Research, 166*, 20–32.

Supplementary materials

Supplementary Movie S1. An example of an RF pattern with constant speed of motion applied to the gratings of the Gabor patches comprising the pattern. For patterns close to threshold modulation, this approximates a constant centrifugal speed. The pattern has three cycles of position and orientation modulation and so the Gabor patches are aligned tangential to the path and the pattern is perceived as a rounded triangle.

Supplementary Movie S2. An example of an RF pattern with a positional modulation applied to the path of Gabor patches but no orientation modulation of their gratings. The gratings of the Gabor patches comprising the pattern have a constant speed of centrifugal motion applied around the patterns.

Supplementary Movie S3. An example of an RF pattern with orientation modulation applied to the Gabor patches but no positional modulation of the path. The gratings of the Gabor patches comprising the pattern again have a constant speed of centrifugal motion.

Supplementary Movie S4. An example of a circular pattern with no modulation of orientation but with an RF modulation of centrifugal speed, a motion RF pattern. The pattern appears to develop an RF shape over time.

Downloaded from hwmaint.iovs.org on 04/25/2024